CORA Cork Open Research Archive
Cartlann Taighde Oscailte Chorcaí

Title	Siponimod as a novel inhibitor of retinal angiogenesis: In vitro and in vivo evidence of therapeutic efficacy
Authors	Alshaikh, Rasha A.;Gamal Eldin Zaki, Rania;Salah El Din, Rania A.;Ryan, Katie B.;Waeber, Christian
Publication date	2023-08-01
Original Citation	Alshaikh, R. A., Gamal Eldin Zaki, R., Salah El Din, R. A., Ryan, K. B. and Waeber, C. (2023) 'Siponimod as a novel inhibitor of retinal angiogenesis: In vitro and in vivo evidence of therapeutic efficacy', Journal of Pharmacology and Experimental Therapeutics, 386(2), pp. 224-241. doi: 10.1124/jpet.122.001529
Type of publication	Article (peer-reviewed)
Link to publisher's version	10.1124/jpet.122.001529
Rights	© 2023, The American Society for Pharmacology and Experimental Therapeutics.
Download date	2026-11-17 12:41:14
Item downloaded from	https://hdl.handle.net/10468/14906

UCC
University College Cork, Ireland
Coláiste na hOllscoile Corcaigh

JPET Fast Forward. Published on May 15, 2023 as DOI: 10.1124/jpet.122.001529
This article has not been copyedited and formatted. The final version may differ from this version.

Siponimod as a novel inhibitor of retinal angiogenesis: *in vitro* and *in vivo* evidence of therapeutic efficacy

Rasha A. Alshaikh [a], Rania Gamal Eldin Zaki [b], Rania A. Salah El Din [c,d] , Katie B. Ryan [a,e], Christian Waeber [a,f]

[a] School of Pharmacy, University College Cork, Cork, Ireland.

[b] Department of Ophthalmology, Faculty of Medicine, Ain Shams University, Cairo, Egypt.

[c] Department of Anatomy and Embryology, Faculty of Medicine, Ain Shams University, Cairo, Egypt.

[d] Department of Anatomy and Embryology, Faculty of Medicine, Newgiza University.

[e] SSPC The SFI Research Centre for Pharmaceuticals, School of Pharmacy, University College Cork, Cork, Ireland

[f] Department of Pharmacology and Therapeutics, University College Cork, Cork, Ireland

Downloaded from jpet.aspetjournals.org at ASPET Journals on June 6, 2023

JPET Fast Forward. Published on May 15, 2023 as DOI: 10.1124/jpet.122.001529
This article has not been copyedited and formatted. The final version may differ from this version.

Running title:

Siponimod as a novel inhibitor of retinal angiogenesis

Corresponding author:

Christian Waeber

address: School of Pharmacy, University College Cork

telephone number: 353(0)214901791

e-mail address: c.waeber@ucc.ie

Document information:

Number of text pages: 26

Number of tables: 1

Number of figures: 8

Number of references: 78

Number of words in the Abstract: 250

Number of words in the Introduction: 617

Number of words in the Discussion: 1395

A list of nonstandard abbreviations:

AMD: Age-related macular degeneration

bFGF: Basic fibroblast growth factor

BrdU: Bromodeoxyuridine

CGM: Complete growth medium

DR: Diabetic retinopathy

DMSO: Dimethyl sulfoxide

FITC: Fluorescein isothiocyanate

FITC-DEX: Fluorescein isothiocyanate-dextran

FBS: Foetal bovine serum

FCS: Foetal calf serum

H&E: Hematoxylin and eosin

HRMEC: Human retinal microvascular endothelial cells

HUVEC: Human umbilical vein endothelial cells

Downloaded from jpet.aspetjournals.org at ASPET Journals on June 6, 2023

JPET Fast Forward. Published on May 15, 2023 as DOI: 10.1124/jpet.122.001529
This article has not been copyedited and formatted. The final version may differ from this version.

MTT: 3-(4,5-dimethylthiazol-2-yl)-2,5-diphenyl-2H-tetrazolium bromide

PBS: Phosphate buffered saline

PET: Polyethylene Terephthalate

RGM: Reduced growth medium

S1P: Sphingosine-1-phosphate

S1PR: Sphingosine-1-phosphate receptor

TEER: Trans endothelial electrical resistance

TCA: trichloroacetic acid

TFA: Trifluoroacetic acid

TNF-α: Tumor necrosis factor–α

VEGF: Vascular endothelial growth factor

Section assignment:

Drug Discovery and Translational Medicine

Downloaded from jpet.aspetjournals.org at ASPET Journals on June 6, 2023

JPET Fast Forward. Published on May 15, 2023 as DOI: 10.1124/jpet.122.001529
This article has not been copyedited and formatted. The final version may differ from this version.

Abstract

S1P receptors control endothelial cell proliferation, migration, and survival. Evidence of the ability of S1P receptor modulators to influence multiple endothelial cell functions suggests their potential use for antiangiogenic effect. The main purpose of our study was to investigate the potential of siponimod for the inhibition of ocular angiogenesis *in vitro* and *in vivo*. We investigated the effects of siponimod on the metabolic activity (MTT assay), cell toxicity (LDH release), basal proliferation and growth factor induced proliferation (BrdU assay), and migration (transwell migration assay) of human umbilical vein endothelial cells (HUVEC) and retinal microvascular endothelial cells (HRMEC). The effects of siponimod on HRMEC monolayer integrity, and barrier function under basal conditions and TNF-α induced disruption were assessed using the trans-endothelial electrical resistance (TEER) and FITC-dextran permeability assays. Siponimod's effect on TNF-α induced distribution of barrier proteins in HRMEC was investigated using immunofluorescence. Finally, the effect of siponimod on ocular neovascularization *in vivo* was assessed using suture-induced corneal neovascularization in albino rabbits.

Our results show that siponimod did not affect endothelial cell proliferation or metabolic activity, but significantly inhibited endothelial cell migration, increased HRMEC barrier integrity, and reduced TNF-α induced barrier disruption. Siponimod also protected against TNF-α induced disruption of claudin-5, ZO-1, and VE-cadherin in HRMEC. These actions are mainly mediated by $S1PR_1$ modulation. Finally, siponimod prevented the progression of suture-induced corneal neovascularization in albino rabbits. In conclusion, the effects of siponimod on various processes known to be involved in angiogenesis support its therapeutic potential in disorders associated with ocular neovascularization.

Downloaded from jpet.aspetjournals.org at ASPET Journals on June 6, 2023

JPET Fast Forward. Published on May 15, 2023 as DOI: 10.1124/jpet.122.001529
This article has not been copyedited and formatted. The final version may differ from this version.

Significance statement

Siponimod is an extensively characterized S1P receptor modulator already approved for the treatment of multiple sclerosis. It inhibited retinal endothelial cell migration, potentiated endothelial barrier function, protected against TNF-α induced barrier disruption, and also inhibited suture-induced corneal neovascularization in rabbits. These results support its use for a novel therapeutic indication in the management of ocular neovascular diseases.

Downloaded from jpet.aspetjournals.org at ASPET Journals on June 6, 2023

JPET Fast Forward. Published on May 15, 2023 as DOI: 10.1124/jpet.122.001529
This article has not been copyedited and formatted. The final version may differ from this version.

Keywords

BAF 312, Diabetes Mellitus, Diabetic Retinopathy, Age-Related Macular Degeneration, Sphingosine 1-phosphate, Corneal Neovascularization.

Downloaded from jpet.aspetjournals.org at ASPET Journals on June 6, 2023

JPET Fast Forward. Published on May 15, 2023 as DOI: 10.1124/jpet.122.001529
This article has not been copyedited and formatted. The final version may differ from this version.

Introduction

Vision impairment affects more than 2.2 billion people around the world. In more than 50% of these cases, it is due to preventable or treatable conditions, such as retinal and choroidal vascular diseases (Bourne *et al.*, 2021). These diseases are characterized by pathological angiogenesis originating from retinal blood vessels (e.g., diabetic retinopathy (DR)) and/or from choroidal blood vessels (e.g., neovascular age-related macular degeneration (AMD)). The newly formed blood vessels are highly unstable, with defective expression of tight junction proteins and smooth muscle and pericyte coverage (Alshaikh *et al.*, 2021). The defective endothelial barrier of these vessels continuously leaks blood and/or blood components, leading to oedema, haemorrhage, and retinal detachment.

Treatment for retinal and/or choroidal neovascular diseases currently relies on angiogenesis inhibitors and to a lesser extent anti-inflammatory corticosteroids. Clinically approved angiogenesis inhibitors for ocular applications mainly include anti-vascular endothelial growth factor (anti-VEGF) therapeutics. VEGF is one of the main growth factors that triggers defective blood vessel formation in ocular diseases. Therefore, anti-VEGF therapy provides a significant improvement in the status of ocular neovascularization. However, anti-VEGF treatments are associated with many limitations including minimal gains in visual acuity (Lotery *et al.*, 2017), stability of the drug, high cost, invasive administration route and multiple side effects. Furthermore, resistance to anti-VEGF treatment, in which patients fail to respond or respond inadequately to anti-VEGF therapy, was reported in 15-40% of cases (Wallsh and Gallemore, 2021). The reason for this resistance is not clearly understood, but may be related to the observation that growth factors other than VEGF can induce angiogenesis and vascular leakage (Cabral *et al.*, 2017; Wallsh and Gallemore, 2021).

Downloaded from jpet.aspetjournals.org at ASPET Journals on June 6, 2023

JPET Fast Forward. Published on May 15, 2023 as DOI: 10.1124/jpet.122.001529
This article has not been copyedited and formatted. The final version may differ from this version.

Hence, there is an unmet need to identify novel pharmacological targets for the management of retinal and choroidal vascular diseases, which could either augment the effects of anti-VEGF agents or exert a beneficial therapeutic action independently of VEGF signalling. Sphingosine 1-phosphate (S1P) is a lipid mediator synthesized and secreted mainly by red blood cells, endothelial cells, and platelets (Proia and Hla, 2015). Significant upregulation of S1P production was observed in retinal cells under stress conditions (Porter *et al.*, 2018; Terao *et al.*, 2019), and in the aqueous humor and serum of diabetic retinopathy patients (Ensari Delioğlu *et al.*, 2021). Extracellular S1P acts through five G-protein coupled receptors, $S1PR_{1\text{-}5}$. $S1PR_1$, $S1PR_2$, and $S1PR_3$ show abundant expression in vascular endothelial cells and have been linked to endothelial cell proliferation, migration, barrier integrity, apoptosis, and inflammation (Swan *et al.*, 2010; Wilkerson and Argraves, 2014). $S1PR_1$ is extensively expressed in endothelial cells and is associated with the maintenance of endothelial barrier function and junctional localization of tight junction proteins (Garcia *et al.*, 2001; Xiong and Hla, 2014). While effects of $S1PR_1$ modulation on endothelial cells were documented previously, the pharmacological characterization of these effects often relied on the use of non-selective agents (e.g., S1P or fingolimod), or agents with unknown specificity (Salomone and Waeber, 2011; Alshaikh *et al.*, 2021). Siponimod has been extensively characterized, showing specificity for $S1PR_1$ and $S1PR_5$ (Gergely *et al.*, 2012). Furthermore, it is already approved for the management of multiple sclerosis (MS). We hypothesized that siponimod may prevent angiogenesis and improve the barrier properties of retinal endothelial cells via $S1PR_1$ modulation. To test our hypothesis, we compared the effects of siponimod on the proliferation and migration of human microvascular retinal endothelial cells (HRMEC) and human umbilical vein endothelial cells (HUVEC). We also assessed siponimod's effects on retinal endothelial barrier integrity by testing transendothelial electrical resistance, FITC-dextran permeability and endothelial junction proteins localization. The effects of a selective

Downloaded from jpet.aspetjournals.org at ASPET Journals on June 6, 2023

JPET Fast Forward. Published on May 15, 2023 as DOI: 10.1124/jpet.122.001529
This article has not been copyedited and formatted. The final version may differ from this version.

$S1PR_1$ antagonist (W146) were also studied to elucidate siponimod's mechanism of action. Finally, as a proof of concept of the antiangiogenic properties of siponimod, we investigated its effects in an *in vivo* corneal angiogenesis model.

Downloaded from jpet.aspetjournals.org at ASPET Journals on June 6, 2023

JPET Fast Forward. Published on May 15, 2023 as DOI: 10.1124/jpet.122.001529
This article has not been copyedited and formatted. The final version may differ from this version.

Materials and methods

Materials

Siponimod hemifumarate and siponimod base were kindly gifted from Novartis pharma AG, Basel, Switzerland. Foetal bovine serum (FBS), penicillin-streptomycin solution, dimethyl sulfoxide (DMSO), trypan blue, methanol, phosphate buffered saline (PBS), thiazolyl blue tetrazolium bromide (3-(4,5-dimethylthiazol-2-yl)-2,5-diphenyltetrazolium bromide) (MTT), cell proliferation ELISA BrdU kit (Roche Diagnostics), recombinant human vascular endothelial growth factor-165 (VEGF), W146 (857390P, Avanti Polar Lipids), trifluoroacetic acid (TFA), Triton™ X-100, trichloroacetic acid (TCA), ammonium hydroxide and crystal violet were purchased from Sigma-Aldrich, Ireland. Normal goat serum blocking solution (Vector Laboratories®, California, USA) was purchased through 2B Scientific Limited, Oxfordshire, United Kingdom. CyQUANT™ LDH Cytotoxicity Assay kit (CAT#C20300), Polyclonal anti-claudin-5 rabbit antibody (Invitrogen, REF# 34-1600), Polyclonal anti ZO-1 rabbit antibody (Invitrogen, REF# 61-7300), Polyclonal anti VE-cadherin rabbit antibody (Invitrogen, REF# 36-1900), and AlexaFlourTM 488 goat anti-rabbit IgG (Invitrogen, REF# A11008, LOT# 2147635 and 2284595) were purchased from Fisher Scientific, Ireland. Human basic fibroblast growth factor (bFGF) was obtained from PromoCell®, Heidelberg, Germany. Carrier-free recombinant human tumour necrosis factor (TNF-α, REF# 210-TA-005) was purchased from R&D Systems, Minneapolis, USA.

Cell culture

Human umbilical vein endothelial cells (HUVEC), low serum endothelial cell growth medium kit (C-22110), and phenol-red free basal medium (C-22215) were purchased from PromoCell®, Heidelberg, Germany. HUVEC were grown and maintained in the complete endothelial cell growth medium recommended by the manufacturer. The medium was supplemented with foetal calf serum (FCS; 2% v/v), endothelial cell growth supplement

Downloaded from jpet.aspetjournals.org at ASPET Journals on June 6, 2023

JPET Fast Forward. Published on May 15, 2023 as DOI: 10.1124/jpet.122.001529
This article has not been copyedited and formatted. The final version may differ from this version.

(ECGS; 0.004 µl/ml), epidermal growth factor (EGF; 0.1 ng/ml), basic fibroblast growth factor (bFGF; 1 ng/ml), heparin (90 µg/ml), hydrocortisone (1 µg/ml) and penicillin-streptomycin (PENSTREP, 1% v/v). The cells were kept in a humidified incubator at 37 °C and 5% CO_2 during all experiments, and studies were conducted using cells from passage number 3 to 7.

In certain experiments, a reduced growth factor medium (RGM) was utilized to reduce the interference from bovine serum components (in particular S1P, present at low micromolar concentrations) (Proia and Hla, 2015). RGM contained one-tenth of the concentrations of all growth supplements in the complete endothelial cell growth medium, except for the PENSTREP concentration which was kept constant at 1% v/v.

Human retinal microvascular endothelial cells (HRMEC) were purchased from CellBiologics®, Chicago, IL, USA. They were grown in a complete human endothelial cell medium supplemented with components from a growth factor supplement kit (REF# H-1168). The growth kit comprised foetal bovine serum (FBS; 5% v/v), EGF (0.1% v/v), FGF (0.1% v/v), VEGF (0.1% v/v), hydrocortisone (0.1% v/v), heparin (0.1% v/v), L-glutamine (1% v/v) and antibiotic-antimycotic solution of penicillin and streptomycin (1% v/v). Before seeding HRMEC in any experiments, the tissue culture flasks, plates, and transwells were coated with a gelatine-based coating solution (REF# 6950, Cell Biologics®) to promote cell adherence. Cells were kept in a humidified incubator maintained at 37 °C and supplemented with 5% CO_2 during all experiments and studies were conducted using cells from passage number 4 to 9. In certain experiments, RGM was employed which contained one-tenth of the concentration of all growth supplements contained in the complete endothelial cell growth medium, except for the antibiotic-antimycotic solution concentration which was kept constant at 1% v/v.

Downloaded from jpet.aspetjournals.org at ASPET Journals on June 6, 2023

JPET Fast Forward. Published on May 15, 2023 as DOI: 10.1124/jpet.122.001529
This article has not been copyedited and formatted. The final version may differ from this version.

Preparation of drug stock solutions

To prepare the stock solution of siponimod hemifumarate, the drug was dissolved in 30% DMSO in PBS and the solution was sonicated for 30 minutes until completely dissolved. The stock solution was diluted to the required concentration in cell culture medium. The DMSO concentration was kept below 0.03% v/v in all cell culture experiments.

W146 was dissolved in 0.4% v/v TFA in methanol before being sonicated for 30 minutes until a clear solution was obtained. The stock solution was diluted to the required concentration in cell culture medium. The concentrations of methanol and TFA in cell culture experiments were kept below 0.5% v/v and 0.0018% v/v, respectively.

Reverse-Transcription Quantitative Polymerase Chain Reaction (RT-qPCR)

RT-qPCR was conducted as described (Fujita *et al.*, 2008). Confluent endothelial cells cultured on six-well plates were harvested and the RNA was extracted and purified using Macherey-Nagel™ NucleoSpin™ RNA, Mini Kit for RNA purification (CAT# 740955.5) following the protocol recommended by the manufacturer. Previously cryopreserved Peripheral Blood Mononuclear Cells (PBMCs) were used as a positive S1pr5 control. They were obtained using a protocol approved by the Clinical Research Ethics Committee of University College Cork [ECM 4 (r) 14/01/2020 and ECM 3 (eee) 08/09/2020] from a control donor who provided written informed consent in accordance with the Declaration of Helsinki. RNA concentration was determined spectrophotometrically before being used to synthesize cDNA using the Applied Biosystems™ High-Capacity cDNA Reverse Transcription Kit (CAT# 4368814) and following the protocol recommended by the supplier. RT-qPCR was performed using a PCR Master Mix (New England Biolabs, Luna Universal Probe qPCR Master Mix, CAT# M3004S) and Applied Biosystems™ TaqMan Gene Expression assay kit for GAPDH (assay ID: Hs99999905_m1), S1pr1(assay ID: Hs00173499_m1) and

Downloaded from jpet.aspetjournals.org at ASPET Journals on June 6, 2023

JPET Fast Forward. Published on May 15, 2023 as DOI: 10.1124/jpet.122.001529
This article has not been copyedited and formatted. The final version may differ from this version.

S1pr5(assay ID: Hs00924881_m1). RT-qPCR analysis was achieved using a CFX96 Touch Real-Time PCR System (Bio-Rad) following the manufacturer protocol. All qPCR measurements were performed in triplicate from three independent replicates. S1pr1 and S1pr5 genes expression was normalized to GAPDH expression, yielding the delta-CT (ΔCt) value which was calculated as follows:

$$\Delta Ct = \text{average Ct of the expression of the gene of interest} - \text{average Ct of GAPDH expression}$$

Thiazolyl Blue Tetrazolium Bromide (MTT) assay

The effects of different drugs on endothelial cell metabolic activity were measured using the MTT assay. HUVEC or HRMEC were seeded at a density of approximately 4×10^3 cells per well in a 96-well plate and were left to adhere overnight in the complete growth medium (CGM). The next day, the culture medium was replaced with a fresh CGM, with or without test drugs, and the cells were incubated for 48 hours in a humidified incubator at 37 °C and 5% CO_2. After the incubation period, MTT solution was added directly to each well to achieve a final concentration of 0.5 mg/ml. The plate was then incubated for 3 hours protected from light in a humidified incubator. After the incubation period, the medium was removed, and the formazan crystals were dissolved with 200 µl of alkaline DMSO solution (containing 800 mM of ammonia) that was added directly to each well. The absorbance was measured at 570 nm using a Wallac Victor 2 plate reader (PerkinElmer®, USA). For each condition, the average absorbance of at least two wells (technical replicates) was used as a single value in the statistical comparison. Each experiment was performed independently at least 4 times ($n \geq 4$).

Lactate dehydrogenase (LDH) release assay

To investigate the toxicity of siponimod and W146 on endothelial cells, LDH release was quantified using Invitrogen CyQUANT™ LDH Cytotoxicity Assay kit. HUVEC or

Downloaded from jpet.aspetjournals.org at ASPET Journals on June 6, 2023

JPET Fast Forward. Published on May 15, 2023 as DOI: 10.1124/jpet.122.001529
This article has not been copyedited and formatted. The final version may differ from this version.

HRMEC were seeded at a density of approximately 10×10^3 cells per well in a 96-well plate and were left to adhere overnight. The next day, the culture medium was replaced with a fresh CGM, with or without test drugs, and the cells were incubated for 48 hours in a humidified incubator at 37 °C and 5% CO_2. After the incubation period, 50 µL of culture medium from each well was transferred to a 96-well flat bottom plate. Then, 50 µL of the reaction mixture was added to each sample and the plates were incubated at room temperature for 30 minutes. After the incubation period, 50 µL of the stop solution was added to each sample before measuring the absorbance immediately at 490 nm. Maximum LDH activity was determined in triplicate wells by adding 10 µL of cell lysis buffer 45 minutes before taking samples from the culture medium. The cytotoxicity (%) was calculated as follows:

$$\text{Cytotoxicity (\%)} = \frac{Treated\ cells\ LDH\ activity - Control\ cells\ LDH\ activity\ (CGM)}{Maximum\ LDH\ activity - Control\ cells\ LDH\ activity\ (CGM)} * 100$$

For each condition, at least two wells (technical replicates) were used, and each experiment was performed independently at least 3 times ($n \geq 3$).

5-Bromo-2′-deoxyuridine (BrdU) incorporation assay

To investigate the effects of different drugs on endothelial cell proliferation, colorimetric quantification of BrdU incorporation into the cell DNA was employed. Endothelial cells (4×10^3 cells per well) were seeded in a 96-well plate and allowed to adhere for at least 10 hours before being starved in RGM overnight. After serum starvation, the medium was replaced by fresh RGM, with or without the test drugs. The cells were then incubated with the drug for 48 hours. BrdU was added to each well to obtain a final concentration of 10 µM and the cells were incubated for 6 hours. Cells were fixed using FixDenat solution before being incubated with the anti-BrdU-peroxidase antibody for 90 minutes at room temperature. The excess antibody was washed using a washing buffer and

Downloaded from jpet.aspetjournals.org at ASPET Journals on June 6, 2023

JPET Fast Forward. Published on May 15, 2023 as DOI: 10.1124/jpet.122.001529
This article has not been copyedited and formatted. The final version may differ from this version.

the cells were incubated with TMB (3,3',5,5'-Tetramethylbenzidine) substrate solution for 20 minutes at room temperature as per the manufacturer's instructions. The absorbance was acquired at 405 nm using a Wallac Victor 2 plate reader (PerkinElmer®, USA). For each condition, the average absorbance of at least two wells (technical replicates) was used as a single value in the statistical comparison. Each experiment was performed independently at least 5 times ($n \geq 5$).

Growth factor-induced cell proliferation

Drug effect on growth factor-induced endothelial cell proliferation was assessed by measuring VEGF- and bFGF-stimulated BrdU incorporation. Approximately 4×10^3 cells were seeded in each well of a 96-well plate and were allowed to adhere overnight. The next day, endothelial cells were starved in endothelial basal medium supplemented with 0.5% v/v FBS for 8-10 hours. After the starvation period, the medium was aspirated and VEGF (40 ng/ml) or bFGF (25 ng/ml), with or without the selected drugs, were introduced in a carrier medium (basal medium supplemented with 1% FBS, 2 µg/ml hydrocortisone). The cells were incubated with the growth factors and the drugs for 72 hours before adding BrdU (final concentration of 10 µM) for a further 6 hours. After incubation with BrdU, a similar protocol was employed as described in the previous section to quantify BrdU incorporation in the cell DNA. Each experiment was performed independently at least 5 times ($n \geq 5$).

Transwell cell migration assay

Endothelial cells (approximately 5×10^4 cells) were seeded in RGM into the upper chamber of a polyethylene terephthalate (PET) transwell insert (pore size 8 µm, Sarstedt, Nümbrecht, Germany) positioned in a 24-well plate. To investigate the effects of S1P receptor modulators on chemotactic signals, the lower chamber was filled with 400 µl of 10% FBS in CGM, VEGF (40 ng/ml) in RGM, or S1P (3µM) in RGM. Drugs (siponimod or

Downloaded from jpet.aspetjournals.org at ASPET Journals on June 6, 2023

JPET Fast Forward. Published on May 15, 2023 as DOI: 10.1124/jpet.122.001529
This article has not been copyedited and formatted. The final version may differ from this version.

W146) were introduced to both the upper and lower chambers simultaneously at the same concentration to eliminate any chemical gradient effects. Cells were allowed to migrate towards the lower chamber for 6 hours before being fixed, stained, and visualized as described below.

In other experiments, S1P receptor modulators were introduced in RGM in the lower chamber to investigate their chemotactic potential and the cells were allowed to migrate towards the lower chamber for 6 hours before being fixed, stained, and visualized. Negative and positive controls employed RGM and 10% FBS in the lower chamber, respectively.

After the cell migration period (6 hours at 37 °C and 5% CO_2), the cell culture inserts were removed and washed, and the membranes were fixed using ice-cold methanol for 25 minutes at 4 °C. The membranes were stained using 0.5% crystal violet for 30 minutes, before the removal of the non-migrating cells on the upper surface using a wet cotton swab. The inserts were left to dry and visualized by light microscopy (BX43 microscope, OLYMPUS®). For each experimental condition, at least 2-3 transwell inserts were employed per experiment. At least two random images were taken per insert, and cells were counted in three random fields in each image.

Wound healing (scratch) assay

HUVEC were seeded at 5 x 10^4 cells per well in a 24-well plate and were incubated until 90% confluency was achieved. The confluent cell monolayer was then scratched using a 200-µl pipette tip, the growth medium was aspirated, and the cell layer was washed twice using PBS to remove any cell debris. Test drugs were introduced in RGM in each well and pictures were acquired immediately (zero-time point) and 12 hours after scratching using an inverted microscope (Leica Microsystems GmbH, Germany). All the pictures for each sample at T= 0 and 12 hours were captured for the same area and the distance between the scratch edges at each time point was measured using ImageJ® software. The rate of cell migration

Downloaded from jpet.aspetjournals.org at ASPET Journals on June 6, 2023

JPET Fast Forward. Published on May 15, 2023 as DOI: 10.1124/jpet.122.001529
This article has not been copyedited and formatted. The final version may differ from this version.

per hour into the wound area (migration distance/migration time in hours) was calculated and used for comparison.

Trans-endothelial electrical resistance (TEER)

TEER was measured using an epithelial volt/ohm meter (World Precision Instruments, Sarasota, FL, USA) using an STX2 chopstick electrode. The experiments were conducted as previously described (Suarez *et al.*, 2014; Srinivasan *et al.*, 2015). Briefly, PET transwell inserts (0.4 μm pore size and 33.6 mm² culture surface area) were positioned in a 24-well plate and were coated with a gelatine-based coating solution for 12-18 hours. The coating solution was aspirated, and the inserts were air dried before seeding the endothelial cells in CGM at a density of 1 x 10^5 cells per insert. The lower chamber was filled with CGM to maintain a consistent liquid level across the membrane. The cells were incubated for 3-4 days, and the medium was changed every other day until a stable TEER of approximately 26 $\pm$ 4 Ohms×cm^2 was obtained. Then, the growth medium was aspirated, the test drug (siponimod or W146) was introduced into the carrier medium (phenol-red free basal medium supplemented with 2% FBS) and the cells were incubated for 48 hours. The TEER was measured at 0, 24, and 48 hours after incubation with the test drugs. In certain experiments, FITC-DEX permeability was assessed at the end of the incubation period as described previously.

In other experiments, after the cells reached a stable TEER of 26 $\pm$ 4 Ohms×cm^2, the medium was aspirated and a new medium (phenol-red free complete growth medium) with human TNF-α (50 ng/ml) was introduced to degrade the endothelial barrier function, with or without test drugs. TEER was recorded at 0, 24, and 48 hours after TNF-α addition. For each experimental condition, at least two transwell inserts were employed per experiment (technical replicates). Each experiment was performed independently at least 5 times ($n \geq 5$). For each transwell insert, the TEER was measured three times at each time point and the

Downloaded from jpet.aspetjournals.org at ASPET Journals on June 6, 2023

JPET Fast Forward. Published on May 15, 2023 as DOI: 10.1124/jpet.122.001529
This article has not been copyedited and formatted. The final version may differ from this version.

average TEER was calculated. The resistance of blank transwell filters was subtracted from the average resistance of each of the experimental inserts and the TEER was calculated by multiplying the resulting net resistance (Ohms) by the surface area of the insert (cm^2), as described in the following equation:

$$TEER\ (Ohms \times Cm^2) = (average\ experimental\ resistance - average\ blank\ resistance) \times membrane\ surface\ area$$

Fluorescein Isothiocyanate-Dextran (FITC-DEX) diffusion

Endothelial cells were grown on PET transwell inserts as described in the TEER assay until a stable resistance of approximately 26 $\pm$ 4 Ohms×cm^2 was obtained. At the end of the incubation period, 40 kDa FITC-DEX was introduced to the top chamber at a final concentration of 0.5 mg/ml. The cells were incubated with FITC-DEX for 2 hours. Then, three samples (100 µL each) were taken from the bottom chamber and one sample (100 µl) from the top chamber. Samples were transferred into a black 96-well plate and the fluorescence was acquired using Wallac Victor 2 plate reader (PerkinElmer®, USA) at 485 nm (excitation) and 535 |nm (emission). The concentration of FITC-DEX in each chamber was calculated using a calibration curve. The apparent permeability coefficient (P_{app}) was calculated as described previously using the following equation (Bernard-Patrzynski *et al.*, 2019):

$$P_{app} = \frac{\frac{dQ}{dT}}{A \times C_0}$$

P_{app} is the apparent permeability coefficient (cm × s^{-1}), dQ is the FITC-DEX amount (µg) in the bottom chamber at a given time dT (seconds), A is the surface area of the transwell insert (cm^2) and C_0 is the concentration of FITC-DEX in the top chamber (µg/ml).

Downloaded from jpet.aspetjournals.org at ASPET Journals on June 6, 2023

JPET Fast Forward. Published on May 15, 2023 as DOI: 10.1124/jpet.122.001529
This article has not been copyedited and formatted. The final version may differ from this version.

Immunocytochemistry of claudin-5, ZO-1 and VE-cadherin

HRMEC (approximately 5 x 10^4 cells) were seeded on a round (13-mm diameter) gelatine-coated glass coverslip placed in a 24-well plate. The cells were grown in CGM for at least 48 hours after reaching confluency. For certain groups, TNF-α (25 ng/ml) only, TNF-α with siponimod (100 nM) or TNF-α with W146 (1 μM) were added to the cells and were incubated for 6 hours before being fixed with 10% ice-cold TCA for 15 minutes. The cells were permeabilized with 0.3% Triton™ X-100 for 15 minutes and blocked with 10% normal goat serum for 30 minutes at room temperature. The samples were then incubated with the primary antibody in 2% normal goat serum at 4 °C overnight. The cell layer was washed before being incubated with AlexaFlour™ 488 goat anti-rabbit antibody (secondary antibody) overnight at 4 °C. At the end of the incubation period, the cells were washed with PBS and the glass coverslips were transferred to a microscope slide before being examined using a light microscope (BX43 microscope, OLYMPUS®). The endothelial junction protein localization and intensity in each image were scored by a blinded researcher considering three features (continuity of the staining in the intercellular junction, the intensity of staining in the intercellular junction, and overall presence of the protein in the intercellular junction). For each feature, the image was scored from 0-4 with 4 being the maximum. At least three random images were taken and ranked for each coverslip, and at least two coverslips per group were employed in each independent replicate. Each experiment was performed independently at least 5 times ($n \geq 5$).

Suture-induced corneal angiogenesis in albino rabbits

A total of 36 adult albino rabbits (50% males and 50% females) weighing approximately 2.2-3 kg were acclimatized for approximately 10 days. All the rabbits were examined and confirmed to have normal avascular corneas prior to surgery. Neovascularization was induced by corneal suturing using a published protocol with

Downloaded from jpet.aspetjournals.org at ASPET Journals on June 6, 2023

JPET Fast Forward. Published on May 15, 2023 as DOI: 10.1124/jpet.122.001529
This article has not been copyedited and formatted. The final version may differ from this version.

modifications (Ucgul *et al.*, 2021). After the acclimatization period, the rabbits were anesthetized using xylazine hydrochloride (i.m., 5 mg/kg) and ketamine hydrochloride (i.v., 35 mg/kg). The right eye of each rabbit was anaesthetized with topical administration of 0.4% benoxinate hydrochloride eye drops. Two 10/0 nylon sutures (Daclon Nylon sutures, SMI, Belgium) were placed at mid-stromal depth, approximately 2 mm from the limbus to induce corneal neovascularization. Suture knots and ends were left exposed to further induce neovascularization and the length of suture end was adjusted to approximately 5 mm. Immediately after the surgery, the rabbits received tobramycin ointment (once) and tobramycin eyedrops (four times daily, for three days). On day 7 after surgery, the corneal neovascularization was confirmed in all rabbits and the rabbits were randomly assigned to one of three groups (n=12) using an online random number generator (https://www.randomizer.org/).

On day 15 after surgery, each rabbit received a 0.1 ml subconjunctival injection into the right eye, approximately 2 mm posterior to the limbus and close to the sutured area. Group A received 0.08% DMSO in PBS (solvent), group B received 5.16 µg/ml siponimod in solvent (low concentration) and group C received 40 µg/ml siponimod in solvent (high concentration). Siponimod in solvent or solvent was injected into the subconjunctival space using a 30-gauge needle on days 15, 18, and 21 (Fig. 9A). Calibrated images were taken on day 15 (before the first dose), and on day 24 (72 hours after the last dose). The neovascular area was manually marked and then measured using ImageJ® software by a researcher blinded to the treatment allocation. At least three images per rabbit were captured at each time point, and the average of the three measurements was employed in the statistical analysis. One rabbit was euthanized before day 24, after reaching a humane endpoint. The data from this rabbit are not included in statistical comparisons.

Downloaded from jpet.aspetjournals.org at ASPET Journals on June 6, 2023

JPET Fast Forward. Published on May 15, 2023 as DOI: 10.1124/jpet.122.001529
This article has not been copyedited and formatted. The final version may differ from this version.

Corneal tissue collection and Haematoxylin and Eosin (H&E) staining

After taking the final images of corneal neovascularization on day 24, rabbits received a final subconjunctival injection of solvent, low concentration siponimod, or high concentration siponimod as described previously. This final dose was administered to observe any acute effect of siponimod on corneal histology. Twelve hours after the final dose, the animals were humanely euthanized with an overdose of ketamine hydrochloride (300 mg/kg) and xylazine hydrochloride (30 mg/kg). The eyeball was surgically enucleated and immediately injected with and stored in 10% buffered formalin for a minimum of 48 hours before histopathological analysis. The eyes were cut, processed, and embedded into paraffin blocks. Sections (5 μm) were mounted onto glass slides for haematoxylin and eosin (H&E) staining to detect gross histopathological abnormalities as described previously (Qiu *et al.*, 2020). Briefly, the ocular sections were dewaxed using two xylene changes, then rehydrated using an ethanol gradient (100% ethanol, 90% ethanol, 70% ethanol) followed by distilled water. The sections were then immersed in haematoxylin stain (BioVision Inc.; prepared as per manufacturer's instructions) before being washed in tap water. Then, the sections were counterstained with eosin before being dehydrated in increasing concentrations of alcohol, followed by two changes of xylene. The sections were then coverslipped and sealed in DPX mounting medium. The images were acquired using an OLYMPUS BX43 microscope (OLYMPUS®, Japan).

Ethical statement and compliance with requirements for studies using animals

The animal study protocols were reviewed and approved by the Animal Experimentation Ethics Committee of University College Cork (Approval number 2022/013) and the Faculty of Medicine, AinShams University (Approval number R3032022A). All experiments were carried out in strict accordance with the European Directive concerning animal experimentation (2010/63/EU). The animal study was reported following the

Downloaded from jpet.aspetjournals.org at ASPET Journals on June 6, 2023

JPET Fast Forward. Published on May 15, 2023 as DOI: 10.1124/jpet.122.001529
This article has not been copyedited and formatted. The final version may differ from this version.

ARRIVE guidelines (Percie du Sert *et al.*, 2020). Albino rabbits were selected as a model for the corneal angiogenesis assay as they provide a higher surface area for corneal suturing compared to rodents, and thus, less variability. The corneal suturing technique was selected to induce angiogenesis as this technique impacts less on animal welfare and relative vision compared to chemical methods of angiogenesis induction (Giacomini *et al.*, 2014). Both male and female rabbits (50% each) were used in each group as per Medical Research Council (MRC) and NC3R recommendations. The sample size (n=12) of each group was calculated using a power analysis (G*power 1.3.9.4 Software) employing F-test, a statistical power of 80%, an alpha level of 0.05, and a Cohen's F of 0.5832 (targeting a minimum meaningful difference of 40% and with a standard deviation of 28%, based on previous studies (Bock *et al.*, 2007; Kim *et al.*, 2008)).

Data analysis

All the data obtained were included in the statistical analysis, and no data points were excluded. For all parametric comparisons, the data are presented as mean $\pm$ standard deviation (SD) and the individual results of each independent replicate are shown when possible. Each independent replicate includes at least two technical replicates, the number of independent replicates (n) is shown in each data presentation. Statistical analysis was conducted using IBM® SPSS® version 28. When needed, the data were normalized for graphical presentation only, but raw non-normalized data were used for statistical comparison. Data were checked for normality using the normal Q-Q plots and formal normality tests when applicable. Randomized block ANOVA (full factorial) was used for statistical comparison of all the experiments except the animal study, for which repeated measures ANOVA was employed. Null hypotheses were rejected for $P < 0.05$. In cases where a statistically significant difference ($P < 0.05$) was obtained in ANOVA, post-hoc (Tukey's multiple comparisons) analysis was conducted. For non-parametric comparisons, Kruskal–

Downloaded from jpet.aspetjournals.org at ASPET Journals on June 6, 2023

JPET Fast Forward. Published on May 15, 2023 as DOI: 10.1124/jpet.122.001529
This article has not been copyedited and formatted. The final version may differ from this version.

Wallis test was employed followed by post-hoc analysis using Dunn's test. Non-parametric data are presented in box plot format showing the minimum, the first-quartile, the median, the third-quartile and the maximum.

Downloaded from jpet.aspetjournals.org at ASPET Journals on June 6, 2023

JPET Fast Forward. Published on May 15, 2023 as DOI: 10.1124/jpet.122.001529
This article has not been copyedited and formatted. The final version may differ from this version.

Results

Siponimod (< 100 nM) does not increase LDH release or reduce the metabolic activity of endothelial cells

The MTT (Fig. 1) and LDH (Fig. 2) assays were used to determine the effects of siponimod and W146 on cell metabolic activity and plasma membrane damage (cytotoxicity), respectively. The different concentration ranges investigated (0.01-10 μM siponimod and 0.1-100 μM W-146) were selected considering their respective IC_{50} of 0.39 nM and 830 nM (Tarrasón *et al.*, 2011; Gergely *et al.*, 2012).

MTT assay results are shown as the average relative absorbance compared to the positive control (CGM), set to 100% in each replicate. Siponimod concentrations up to 100 nM did not significantly affect the metabolic activity of HUVEC (Fig. 1A) or HRMEC (Fig. 1C) compared to CGM. Higher siponimod concentrations (1 and 10 μM) decreased metabolic activity in HUVEC, indicating possible toxicity. The selective $S1PR_1$ antagonist W146 did not affect the metabolic activity of HUVEC (Fig. 1B) or HRMEC (Fig. 1D) at concentrations up to 10 μM, but the metabolic activity of both cell lines significantly dropped in the presence of 100 μM W146. Based on these MTT results, all cell culture experiments used siponimod and W146 at doses equal to or less than 100 nM and 10 μM, respectively.

LDH assay results are presented as % cytotoxicity in HUVEC (in Fig. 2A and Fig. 2B) and in HRMEC (Fig. 2C and Fig. 2D). Siponimod and W146 (100 μM) significantly increased LDH release in both cell lines, confirming the toxic effect of higher drug concentration, while lower concentration had no significant effect.

Siponimod does not affect endothelial cell proliferation

Endothelial cell proliferation is the first step of both physiological and pathological angiogenesis (Alshaikh *et al.*, 2021). To examine the effect of siponimod on basal

Downloaded from jpet.aspetjournals.org at ASPET Journals on June 6, 2023

JPET Fast Forward. Published on May 15, 2023 as DOI: 10.1124/jpet.122.001529
This article has not been copyedited and formatted. The final version may differ from this version.

proliferation, the drug was introduced in RGM to reduce interference from growth factors in the CGM. Siponimod (1 nM to 100 nM) resulted in no noticeable effect on HUVEC or HRMEC proliferation (Fig. 3A and Fig. 3C). Similarly, blocking $S1PR_1$ signalling with W146 did not affect HUVEC and HRMEC proliferation (Fig. 3B and Fig.3D). The positive control (CGM) induced robust proliferation in both cell lines.

VEGF levels in the vitreous and blood of patients with proliferative diabetic retinopathy are higher than in a normal population (Wang *et al.*, 2014), and VEGF is known to induce $S1PR_1$ expression in endothelial cells (Igarashi *et al.*, 2003). Similarly, bFGF concentration is higher in diabetic retinopathy patients (Kon *et al.*, 1999; Jonas and Neumaier, 2007; Bromberg-White *et al.*, 2013; Li *et al.*, 2015). The mitogenic effects of bFGF on vascular smooth muscle cells, astrocytes and auditory neuroblasts are mediated by sphingosine kinase and autocrine/paracrine S1P receptor signaling (Xu *et al.*, 2002; Bassi *et al.*, 2006; Bruno *et al.*, 2017). Similarly, non-mitogenic FGF1 promotes angiogenesis in post-stroke brain and human brain microvascular endothelial cells via S1PR1 upregulation and activation(Zou *et al.*, 2020). Therefore, we characterized the effects of siponimod on endothelial cell proliferation when cells were grown in the presence of bFGF (25 ng/ml) or VEGF (40 ng/ml). Both growth factors were introduced in a reduced-serum carrier medium (basal medium supplemented with 1% FBS and 2 µg/ml hydrocortisone). The UV/VIS absorbance of cells in the carrier medium was set to 100% and the data are presented as a % of the carrier medium absorbance for data visualization. Siponimod (100 nM) and W146 (10 µM) did not affect basal cell proliferation. While siponimod (1-100 nM) did not affect the proliferation of endothelial cells stimulated with 25 ng/ml bFGF (HUVEC in Fig. 4A and HRMEC in Fig. 4C), W146 (10 µM) resulted in a statistically significant reduction in the proliferation of bFGF-stimulated HUVEC and HRMEC as shown in Fig. 4B and Fig. 4D, respectively.

Downloaded from jpet.aspetjournals.org at ASPET Journals on June 6, 2023

JPET Fast Forward. Published on May 15, 2023 as DOI: 10.1124/jpet.122.001529
This article has not been copyedited and formatted. The final version may differ from this version.

The effects on VEGF-stimulated proliferation were comparable (Fig. 5). Siponimod did not significantly inhibit VEGF-induced proliferation of HUVEC or HRMEC (Fig. 5A and Fig. 5C), while 10 μM W146 resulted in statistically significant inhibition of the proliferation of VEGF-stimulated HUVEC (Fig. 5B) and HRMEC (Fig. 5D). Both 0.1 and 1 μM W146 inhibited the proliferation of VEGF-stimulated HRMEC. The ability of W146 to inhibit both bFGF and VEGF-induced endothelial cell proliferation is unlikely to be due to toxicity as 10 μM W146 did not alter the proliferation of non-stimulated endothelial cells.

Siponimod inhibits endothelial cell migration in a dose-dependent manner, possibly via $S1PR_1$ antagonism

Endothelial cell migration is a key event in pathological neovascularization (Caldwell *et al.*, 2003; Lamalice *et al.*, 2007). In transwell migration assays, siponimod (1-100 nM) dose-dependently inhibited HUVEC (Fig. 6A) and HRMEC migration (Fig. 6D) toward 10% FBS. The maximum inhibition was seen with 100 nM siponimod which inhibited cell migration by 70.4% (HUVEC) and 61.1% (HRMEC). Similarly, W146 dose-dependently inhibited HUVEC (Fig. 6B) and HRMEC (Fig. 6E) migration. Siponimod also significantly inhibited cell migration towards S1P (3 μM) and VEGF (40 ng/ml). These effects were also seen with W146 suggesting the $S1PR_1$ antagonism is responsible for the inhibitory actions. The production of both VEGF and S1P is upregulated in retinal injury, and inhibiting migration toward both chemoattractants can be of clinical significance (Wang *et al.*, 2014; Eresch *et al.*, 2018; Terao *et al.*, 2019).

Previous reports suggest that $S1PR_1$ modulators on their own stimulate endothelial cell migration (Sartawi *et al.*, 2020). To further characterize the effects of siponimod on endothelial cell chemotaxis, the transwell migration assay was conducted under reduced growth factor conditions, using only RGM with or without siponimod in the lower chamber,

Downloaded from jpet.aspetjournals.org at ASPET Journals on June 6, 2023

JPET Fast Forward. Published on May 15, 2023 as DOI: 10.1124/jpet.122.001529
This article has not been copyedited and formatted. The final version may differ from this version.

to test migration toward this agent. In the absence of growth factors, siponimod acted as a chemoattractant for both HUVEC and HRMEC (Supplementary Fig. 1). Unlike the inhibitory effect on growth factor-induced migration, W146 did not result in a significant change in endothelial cell migration in the absence of growth factors. Similar to what was observed in the transwell assay, siponimod increased endothelial cell migration into the wound area under reduced growth factor conditions, whereas W146 had no effect (Supplementary Fig. 2).

Siponimod potentiates retinal endothelial barrier integrity and protects against TNF-α induced barrier disruption

The effects of siponimod on retinal endothelial barrier function were investigated by measuring TEER and FITC-DEX permeability. Siponimod potentiates the endothelial barrier integrity under basal conditions, as shown by the increase in TEER after 24 and 48 hours of siponimod application (Fig. 7A). Correspondingly, siponimod reduced the FITC-DEX flux across the endothelial monolayer after 48 hours of incubation (Fig. 7B). W146 had no significant effect on endothelial barrier function assessed by either TEER or FITC-DEX permeability.

TNF-α is a key inflammatory mediator that increases retinal vascular permeability and disrupts endothelial junctions (Zhang *et al.*, 2017). Its levels are higher in the vitreous of patients with AMD and DR (Spranger *et al.*, 1995; Suzuki *et al.*, 2011). TNF-α was also associated with reduced claudin-5 and zonula occludens-1 (ZO-1) expression (Aveleira *et al.*, 2010). The reduction and redistribution of claudin-5 are characteristic of resistant diabetic macular oedema (DME) (Arima *et al.*, 2020) and AMD (Hudson *et al.*, 2019). The retinal endothelial monolayer was therefore challenged with TNF-α (50 ng/ml), a concentration that did not affect the viability of retinal endothelial cells (data not shown). TNF-α resulted in a statistically significant reduction in the TEER of the HRMEC monolayer and a significant

Downloaded from jpet.aspetjournals.org at ASPET Journals on June 6, 2023

JPET Fast Forward. Published on May 15, 2023 as DOI: 10.1124/jpet.122.001529
This article has not been copyedited and formatted. The final version may differ from this version.

increase in FITC-DEX flux (Fig. 7C and Fig. 7D). Siponimod (100 nM) reduced TNF-α induced barrier disruption as reflected by the restoration of TEER values and FITC-DEX permeability (Fig. 7C and Fig. 7D). The $S1P_1$ receptor antagonist W146 (10 μM) was ineffective (Fig. 7C and Fig. 7D).

Siponimod protects against TNF-α induced disruption of endothelial junction proteins in retinal endothelial cells

Disrupted endothelial junction proteins are critical components in retinal endothelial barrier dysfunction (Gardner, 1995; Nakamura *et al.*, 2012). HRMEC showed characteristic expression of claudin-5, ZO-1 and VE-cadherin with continuous junctional localization under control complete growth medium (CGM) conditions (single arrowheads in Fig. 8D). Incubation with TNF-α (25 ng/ml) for 6 hours resulted in reduced expression and disrupted membrane localization of claudin-5 (double arrowhead in Fig. 8D). Similarly, TNF-α treatment reduced the presence and disrupted the localization of ZO-1 and VE-cadherin in retinal endothelial cells (Fig. 8D). The disrupted expression of the endothelial junction protein was reflected by the lower staining scores compared to the untreated controls (Fig. 8A, Fig. 8B, and Fig. 8C). TNF-α-treated cells incubated with siponimod (100 nM) showed a partially recovered expression of claudin-5, ZO-1 and VE-cadherin and higher localization into the intercellular junction (single arrowhead in Fig. 8D). This was reflected by the higher score obtained from siponimod-treated cells compared to TNF-α treatments without siponimod. On the contrary, cells incubated with W146 (10 μM) and TNF-α showed disrupted junctional localization and reduced overall presence of claudin-5, ZO-1, and VE-cadherin (double arrowhead in Fig. 8D). Therefore, W146 did not protect against TNF-α induced changes.

Downloaded from jpet.aspetjournals.org at ASPET Journals on June 6, 2023

JPET Fast Forward. Published on May 15, 2023 as DOI: 10.1124/jpet.122.001529
This article has not been copyedited and formatted. The final version may differ from this version.

Siponimod inhibits the progression of corneal neovascularization in albino rabbits

Corneal neovascularization models are commonly used to predict the antiangiogenic potential of novel drugs (Kather and Kroll, 2014). Corneal neovascularization was induced in albino rabbits by inserting two 10/0 nylon sutures into the avascular corneal area. Animals received three subconjunctival injections of 100 µL solution with a low or high siponimod concentration (5.16 µg/ml or 40 µg/ml) (Fig. 9A). Both concentrations significantly reduced the growth of the neovascular area compared to the solvent group. The mean neovascular areas for the animals in the solvent control group, low concentration siponimod group, and high concentration siponimod group were 8.8 $\pm$ 3.3 mm^2, 8.2 $\pm$ 3.9 mm^2, and 8.3 $\pm$ 2.9 mm^2 on day zero (before the first dose). On day 9 (72 hours after the third dose), animals receiving the solvent showed a mean neovascular area of 14.7 $\pm$ 6.6 mm^2 compared to 7.4 $\pm$ 2.4 mm^2 and 5.7 $\pm$ 2.5 mm^2 in animals receiving low and high doses of siponimod, respectively (Fig. 9B). These results indicate that siponimod produced a significant antiangiogenic effect inhibiting the growth of corneal neovascularization in rabbits. Furthermore, H&E staining of rabbit corneas receiving solvent treatment showed infiltration of inflammatory cells and distortion of the stromal matrix. These histopathological changes were less noticeable in rabbits receiving low and high concentrations of siponimod (Fig. 9D). Furthermore, significant fracturing and thinning of the epithelium were noticed in the rabbits receiving the solvent compared to the siponimod-treated rabbits. The mean epithelium thickness was 11.2 $\pm$ 1.5 µm in solvent-treated corneas, compared to the 11.6 $\pm$ 2.5 µm (low concentration) and 14.6 $\pm$ 2.3 µm (high concentration siponimod).

Downloaded from jpet.aspetjournals.org at ASPET Journals on June 6, 2023

JPET Fast Forward. Published on May 15, 2023 as DOI: 10.1124/jpet.122.001529
This article has not been copyedited and formatted. The final version may differ from this version.

Discussion

The main finding of this study is that siponimod is effective in reducing several processes known to play a key role in retinal neovascularization (i.e, endothelial cell migration, TNF-α induced barrier dysfunction and junctional proteins redistribution). Additionally, siponimod inhibited corneal neovascularization *in vivo*.

S1P receptors control endothelial cell functions that affect physiological and pathological blood vessel formation and therefore represent important targets for neovascular diseases. To validate $S1PR_1$ modulation as therapeutic target for the management of retinal neovascularization, we tested siponimod and W146 at concentrations commonly used in *in vitro* experiments (Liu et al., 2015; Lupino et al., 2019; Spampinato et al., 2021; Wang et al., 2022) and based on their potency at $S1PR_1$ (Tarrasón *et al.*, 2011; Gergely *et al.*, 2012). Endothelial cells express $S1PR_{1-3}$ (Xiong and Hla, 2014). Of relevance to this study, this expression profile is well-documented for HUVEC (Paik *et al.*, 2001; Krump-Konvalinkova *et al.*, 2005; Zheng *et al.*, 2019) and HRMEC (Caballero *et al.*, 2009; Du *et al.*, 2012). Our RT-qPCR analysis agrees with these data, with a prominent expression of S1pr1 and no detected S1pr5 in HUVEC and HRMEC (Supplementary Table 1). The pharmacological profile of siponimod and the absence of $S1P_5$ receptors in these cells therefore indicate that the effects of siponimod in this study are mediated by $S1PR_1$.

The mode of action of siponimod in MS is thought to involve agonist-induced internalization of $S1P_1$ receptors on lymphocytes, i.e. functional antagonism (Scott, 2020). The effects of siponimod could therefore be due to simple agonist effects or functional antagonism, since S1P was likely present in most of our experiments, either from the added serum, or synthesized by endothelial cells (Table 1) (Maines *et al.*, 2006b). In an attempt to differentiate between the two possibilities, we compared the effects of siponimod with those

Downloaded from jpet.aspetjournals.org at ASPET Journals on June 6, 2023

JPET Fast Forward. Published on May 15, 2023 as DOI: 10.1124/jpet.122.001529
This article has not been copyedited and formatted. The final version may differ from this version.

of the $S1PR_1$ antagonist W146 in all *in vitro* experiments (Table 1) (Gonzalez-Cabrera *et al.*, 2008). Our results suggest that inhibition of endothelial cell chemotaxis toward serum components, VEGF, and S1P was due to $S1PR_1$ antagonism, either functional or direct, as both siponimod and W146 had the same effect (Table 1). For growth factor-induced proliferation, only W146 showed an effect. This is likely because cell proliferation induced by either bFGF or VEGF is sphingosine kinase dependent and may involve $S1PR_1$ (Shu *et al.*, 2002; Maines *et al.*, 2006a; Bruno *et al.*, 2017). We hypothesize that W146 fully blocks these receptors, preventing inside-out signalling by S1P (Takabe *et al.*, 2008), whereas $S1PR_1$ downregulated by siponimod may continue to mediate some of the effects of S1P (Mullershausen *et al.*, 2009). In absence of added S1P, cells migrated toward siponimod, but not W146. Cell migration toward siponimod (Sartawi *et al.*, 2020), SEW2871 and fingolimod (Eken *et al.*, 2019) was previously reported, suggesting the importance of $S1PR_1$ activation in this response. Finally, the barrier-protective effect of siponimod, not observed with W146, agrees with recent reports that attribute endothelial barrier enhancement by siponimod to $S1PR_1$ activation through PI3K/Akt pathway (Spampinato *et al.*, 2021). Similarly, $S1PR_1$ activation by siponimod attenuates the apoptosis of retinal ganglion cells via Akt and Erk1/2 activation (Basavarajappa *et al.*, 2023).

Neovascularization in retinal and choroidal vascular diseases involves endothelial cell proliferation, migration, and sprouting assembly (Naito *et al.*, 2020). In our study, neither siponimod nor W146 affected endothelial cell proliferation in the absence of exogenous growth factors. While some studies suggest that $S1PR_1$ activation stimulates cell proliferation (Kimura *et al.*, 2000; Rikitake *et al.*, 2002; O'Sullivan and Dev, 2013), siponimod was shown previously to produce no effect on the proliferation of HUVEC (Sartawi *et al.*, 2020), dermal vascular endothelial cells and pulmonary vascular endothelial cells (Pognan *et al.*, 2018). Although endothelial cell proliferation is an essential step in angiogenesis, a lack of an effect

Downloaded from jpet.aspetjournals.org at ASPET Journals on June 6, 2023

JPET Fast Forward. Published on May 15, 2023 as DOI: 10.1124/jpet.122.001529
This article has not been copyedited and formatted. The final version may differ from this version.

on this parameter does not preclude therapeutic effectiveness. Indeed, bevacizumab does not affect the basal proliferation of retinal endothelial cells (Deissler *et al.*, 2012).

We showed that siponimod inhibited chemotactic endothelial cell migration towards serum, S1P, and VEGF, another key step in angiogenesis (Lamalice *et al.*, 2007). In the presence of added growth factors, the effect of siponimod is likely mediated by antagonistic activity on $S1PR_1$ as W146 also inhibited endothelial cell migration. Siponimod's ability to inhibit HUVEC migration was reported previously using the wound healing assay (Gong *et al.*, 2021). Inhibition of VEGF-induced endothelial cell migration was also observed following $S1PR_1$ antagonism with TASP0277308 (Fujii *et al.*, 2012).

Interestingly, both $S1PR_1$ agonists and antagonists can inhibit angiogenesis in certain models. Indeed, the $S1PR_1$ agonist SEW2871 mimicked the antiangiogenic effects of fingolimod ($S1PR_1$, $S1PR_3$, $S1PR_4$ and $S1PR_5$ modulator) by inhibiting sprouting angiogenesis in HUVEC spheroids (Schmid *et al.*, 2007). SEW2871 also showed an antiangiogenic activity on ovarian transplants in mice (Soleimani *et al.*, 2011). While other reports show that SEW2871 holds a pro-angiogenic effect, by acting as a chemoattractant to CHO cells (Germana Sanna *et al.*, 2004).

Newly formed blood vessels in ocular neovascular diseases are characterised by defective endothelium, improper smooth muscle cell recruitment, and pericyte activation. The defective endothelium results in uncontrolled leakage to the surrounding tissue resulting in progressive macular oedema and vitreous haemorrhage (Krock *et al.*, 2011). Anti-VEGF therapeutics fail to provide long-term protection against retinal endothelial permeability (Deissler *et al.*, 2022), suggesting that novel therapeutics improving barrier function may have benefits. TNF-α is a key inflammatory mediator that increases retinal vascular permeability and disrupts endothelial junctions (Zhang *et al.*, 2017). Hence, we used TNF-α

Downloaded from jpet.aspetjournals.org at ASPET Journals on June 6, 2023

JPET Fast Forward. Published on May 15, 2023 as DOI: 10.1124/jpet.122.001529
This article has not been copyedited and formatted. The final version may differ from this version.

to induce barrier breakdown and disrupt claudin-5, ZO-1, and VE-cadherin distribution in retinal endothelial cells. Our results show that siponimod potentiates the resting barrier function and prevents TNF-α-induced barrier disruption. These protective actions of siponimod on the endothelial barrier do not seem to be mediated by functional S1PR antagonism, since W146 does not show these effects in our experiments. Our experiments also showed that siponimod, but not W146, increases claudin-5, ZO-1, and VE-cadherin localization to the intercellular junction and prevents the disruption of the assembly after TNF-α exposure. These findings agree with the reported barrier-protective effects of siponimod on brain microvascular endothelial cells/astrocytes co-cultures as the drug potentiated the barrier function and prevented interferon γ (IFNγ)/TNFα -induced barrier disruption (Spampinato *et al.*, 2021). Siponimod has also been shown to enhance BBB barrier fuction by acting on other cell types (Spampinato *et al.*, 2022). The lack of effect of W146 in our studies seems to fully reproduce the disruptive effects of $S1PR_1$ blockers on the endothelial barrier reported previously for W146 on HUVEC (Jeya Paul *et al.*, 2020) and for VPC23019 ($S1PR_1$ and $S1PR_3$ antagonist) on retinal endothelial cells (McGuire *et al.*, 2011).

Findings obtained with siponimod add to the body of literature showing that $S1PR_1$ activation improves the endothelial barrier (Wilkerson and Argraves, 2014; Golding-Ochsenbein *et al.*, 2019). Evidence is however more conflicting regarding the effect of fingolimod on endothelial barrier function. This modulator, less specific than siponimod, was shown to protect against barrier disruption of brain microvascular endothelial cells (BMEC) (Nishihara *et al.*, 2015) and of the blood-retinal barrier (Copland *et al.*, 2012). But other data suggest that fingolimod does not affect the barrier function of BMEC (Schuhmann *et al.*, 2015) or is even associated with increased BBB permeability (Yanagida *et al.*, 2017). Potential differences between the effects of siponimod and fingolimod on endothelial barrier function and possible underlying mechanisms require further investigations.

Downloaded from jpet.aspetjournals.org at ASPET Journals on June 6, 2023

JPET Fast Forward. Published on May 15, 2023 as DOI: 10.1124/jpet.122.001529
This article has not been copyedited and formatted. The final version may differ from this version.

Finally, we established the antiangiogenic effects of siponimod in the corneal neovascularization model in albino rabbits. This model was selected to test siponimod's effect specifically on the angiogenic component of ocular diseases (Chang *et al.*, 2012). Corneal neovascularization uses a similar VEGF-dependent angiogenic cascade as the retinal and choroidal neovascularization and has previously been used to establish the therapeutic potential of bevacizumab (Gan *et al.*, 2004; Avisar *et al.*, 2010; Eski *et al.*, 2022), ranibizumab (Dratviman *et al.*, 2008; Eski *et al.*, 2022), and aflibercept (Park and Chung, 2015; Gore *et al.*, 2021). Both siponimod concentrations resulted in a significantly smaller neovascular area after 9 days of treatment. The tested concentrations of 5.16 µg/ml and 40 µg/ml represent 25,000 and 200,000 times the IC_{50} of siponimod on $S1PR_1$ (Gergely *et al.*, 2012). This high ratio (tested dose to published *in vitro* potency) was based on studies that investigated the antiangiogenic effect of small molecules in the same model (Ko *et al.*, 2013; Lledó Riquelme *et al.*, 2018). The ability of siponimod to inhibit corneal neovascularization provides sufficient evidence for therapeutic antiangiogenic actions.

Conclusion

In conclusion, the main findings of our study are that siponimod was able to inhibit endothelial cell migration and reduce the TNF-α induced endothelial barrier dysfunction *in vitro* and inhibit corneal neovascularization *in vivo*. Whilst siponimod does not affect endothelial cell proliferation, the other effects on cell migration, barrier integrity, and claudin expression strongly suggest a potential for antiangiogenic action in neovascular retinal diseases. Further studies are required to establish the effects of siponimod in retinal and choroidal neovascularization disease models and to establish a suitable formulation for the therapeutic management of these disorders.

Downloaded from jpet.aspetjournals.org at ASPET Journals on June 6, 2023

JPET Fast Forward. Published on May 15, 2023 as DOI: 10.1124/jpet.122.001529
This article has not been copyedited and formatted. The final version may differ from this version.

Authorship Contributions

Participated in research design: Rania Gamal Eldin Zaki, Rania A. Salah El Din, Katie B. Ryan, Christian Waeber

Conducted experiments*:* Rasha A. Alshaikh

Contributed new reagents or analytic tools: Katie B. Ryan, Christian Waeber

Performed data analysis*:* Rasha A. Alshaikh, Katie B. Ryan, Christian Waeber

Wrote or contributed to the writing of the manuscript: Rasha A. Alshaikh, Katie B. Ryan, Christian Waeber

Downloaded from jpet.aspetjournals.org at ASPET Journals on June 6, 2023

JPET Fast Forward. Published on May 15, 2023 as DOI: 10.1124/jpet.122.001529
This article has not been copyedited and formatted. The final version may differ from this version.

Footnotes

This work was funded by the Irish Research Council (IRC), project ID [GOIPG/2020/971]

No author has an actual or perceived conflict of interest with the contents of this article.

Reprint request to be sent to the corresponding author

Prof Christian Waeber

School of Pharmacy

University College Cork

Email: c.waeber@ucc.ie

Data Availability Statement

All the data that support the findings of this study are available on request from the corresponding author.

Downloaded from jpet.aspetjournals.org at ASPET Journals on June 6, 2023

JPET Fast Forward. Published on May 15, 2023 as DOI: 10.1124/jpet.122.001529
This article has not been copyedited and formatted. The final version may differ from this version.

References

Alshaikh RA, Ryan KB, and Waeber C (2021) Sphingosine 1-phosphate, a potential target in neovascular retinal disease. *Br J Ophthalmol* **0**:1–9, BMJ Publishing Group Ltd.

Arima M, Nakao S, Yamaguchi M, Feng H, Fujii Y, Shibata K, Wada I, Kaizu Y, Ahmadieh H, Ishibashi T, Stitt AW, and Sonoda KH (2020) Claudin-5 Redistribution Induced by Inflammation Leads to Anti-VEGF–Resistant Diabetic Macular Edema. *Diabetes* **69**:981–999, American Diabetes Association.

Aveleira CA, Lin CM, Abcouwer SF, Ambrósio AF, and Antonetti DA (2010) TNF-α Signals Through PKCζ/NF-κB to Alter the Tight Junction Complex and Increase Retinal Endothelial Cell Permeability. *Diabetes* **59**:2872, American Diabetes Association.

Avisar I, Weinberger D, and Kremer I (2010) Effect of subconjunctival and intraocular bevacizumab injections on corneal neovascularization in a mouse model. *Curr Eye Res* **35**:108–115, Curr Eye Res.

Basavarajappa D, Gupta VV, Wall R Vander, Gupta VV, Chitranshi N, Mirshahvaladi SSO, Palanivel V, You Y, Mirzaei M, Klistorner A, and Graham SL (2023) S1PR1 signaling attenuates apoptosis of retinal ganglion cells via modulation of cJun/Bim cascade and Bad phosphorylation in a mouse model of glaucoma. **37**:e22710.

Bassi R, Anelli V, Giussani P, Tettamanti G, Viani P, and Riboni L (2006) Sphingosine-1-phosphate is released by cerebellar astrocytes in response to bFGF and induces astrocyte proliferation through Gi-protein-coupled receptors. *Glia* **53**:621–630, John Wiley & Sons, Ltd.

Bernard-Patrzynski F, Lécuyer MA, Puscas I, Boukhatem I, Charabati M, Bourbonnière L, Ramassamy C, Leclair G, Prat A, and Roullin VG (2019) Isolation of endothelial cells,

Downloaded from jpet.aspetjournals.org at ASPET Journals on June 6, 2023

JPET Fast Forward. Published on May 15, 2023 as DOI: 10.1124/jpet.122.001529
This article has not been copyedited and formatted. The final version may differ from this version.

pericytes and astrocytes from mouse brain. *PLoS One* **14**, Public Library of Science.

Bock F, Onderka J, Dietrich T, Bachmann B, Kruse FE, Paschke M, Zahn G, and Cursiefen C (2007) Bevacizumab as a Potent Inhibitor of Inflammatory Corneal Angiogenesis and Lymphangiogenesis. *Invest Ophthalmol Vis Sci* **48**:2545–2552, The Association for Research in Vision and Ophthalmology.

Bourne RRA, Steinmetz JD, Saylan M, Mersha AM, Weldemariam AH, Wondmeneh TG, Sreeramareddy CT, Pinheiro M, Yaseri M, Yu C, Zastrozhin MS, Zastrozhina A, Zhang ZJ, Zimsen SRM, Yonemoto N, Tsegaye GW, Vu GT, Vongpradith A, Renzaho AMN, Sorrie MB, Shaheen AA, Shiferaw WS, Skryabin VY, Skryabina AA, Saya GK, Rahimi-Movaghar V, Shigematsu M, Sahraian MA, Naderifar H, Sabour S, Rathi P, Sathian B, Miller TR, Rezapour A, Rawal L, Pham HQ, Parekh U, Podder V, Onwujekwe OE, Pasovic M, Otstavnov N, Negash H, Pawar S, Naimzada MD, Al Montasir A, Ogbo FA, Owolabi MO, Pakshir K, Mohammad Y, Moni MA, Nunez-Samudio V, Mulaw GF, Naveed M, Maleki S, Michalek IM, Misra S, Swamy SN, Mohammed JA, Flaxman S, Park EC, Briant PS, Meles GG, Hayat K, Landires I, Kim GR, Liu X, LeGrand KE, Taylor HR, Kunjathur SM, Khoja TAM, Bicer BK, Khalilov R, Hashi A, Kayode GA, Carneiro VLA, Kavetskyy T, Kosen S, Kulkarni V, Holla R, Kalhor R, Jayaram S, Islam SMS, Gilani SA, Eskandarieh S, Molla MD, Itumalla R, Farzadfar F, Congdon NG, Elhabashy HR, Elayedath R, Couto RAS, Dervenis N, Cromwell EA, Dahlawi SMA, Resnikoff S, Casson RJ, Abdoli A, Choi JYJ, et al. (2021) Causes of blindness and vision impairment in 2020 and trends over 30 years, and prevalence of avoidable blindness in relation to VISION 2020: the Right to Sight: an analysis for the Global Burden of Disease Study. **9**.

Bromberg-White JL, Glazer L, Downer R, Furge K, Boguslawski E, and Duesbery NS (2013)

Downloaded from jpet.aspetjournals.org at ASPET Journals on June 6, 2023

JPET Fast Forward. Published on May 15, 2023 as DOI: 10.1124/jpet.122.001529
This article has not been copyedited and formatted. The final version may differ from this version.

Identification of VEGF-Independent Cytokines in Proliferative Diabetic Retinopathy Vitreous. *Invest Ophthalmol Vis Sci* **54**:6472–6480, The Association for Research in Vision and Ophthalmology.

Bruno M, Rizzo IM, Romero-Guevara R, Bernacchioni C, Cencetti F, Donati C, and Bruni P (2017) Sphingosine 1-phosphate signaling axis mediates fibroblast growth factor 2-induced proliferation and survival of murine auditory neuroblasts. *Biochim Biophys Acta - Mol Cell Res* **1864**:814–824, Elsevier.

Caballero S, Swaney J, Moreno K, Afzal A, Kielczewski J, Stoller G, Cavalli A, Garland W, Hansen G, Sabbadini R, and Grant MB (2009) Anti-sphingosine-1-phosphate monoclonal antibodies inhibit angiogenesis and sub-retinal fibrosis in a murine model of laser-induced choroidal neovascularization. *Exp Eye Res* **88**:367, NIH Public Access.

Cabral T, Mello LGM, Lima LH, Polido J, Regatieri C V., Belfort R, and Mahajan VB (2017) Retinal and choroidal angiogenesis: a review of new targets. *Int J Retin Vitr 2017 31* **3**:1–13, BioMed Central.

Caldwell RB, Bartoli M, Behzadian MA, El-Remessy AEB, Al-Shabrawey M, Platt DH, and Caldwell RW (2003) Vascular endothelial growth factor and diabetic retinopathy: pathophysiological mechanisms and treatment perspectives. *Diabetes Metab Res Rev* **19**:442–455, John Wiley & Sons, Ltd.

Chang JH, Garg NK, Lunde E, Han KY, Jain S, and Azar DT (2012) Corneal Neovascularization: An Anti-VEGF Therapy Review. *Surv Ophthalmol* **57**:415, NIH Public Access.

Copland DA, Liu J, Schewitz-Bowers LP, Brinkmann V, Anderson K, Nicholson LB, and Dick AD (2012) Therapeutic Dosing of Fingolimod (FTY720) Prevents Cell Infiltration, Rapidly Suppresses Ocular Inflammation, and Maintains the Blood-Ocular Barrier. *Am J*

Downloaded from jpet.aspetjournals.org at ASPET Journals on June 6, 2023

JPET Fast Forward. Published on May 15, 2023 as DOI: 10.1124/jpet.122.001529
This article has not been copyedited and formatted. The final version may differ from this version.

Pathol **180**:672–681, Elsevier.

Deissler HL, Deissler H, and Lang GE (2012) Actions of bevacizumab and ranibizumab on microvascular retinal endothelial cells: similarities and differences. *Br J Ophthalmol* **96**:1023–1028, BMJ Publishing Group Ltd.

Deissler HL, Rehak M, Busch C, and Wolf A (2022) Blocking of VEGF-A is not sufficient to completely revert its long-term effects on the barrier formed by retinal endothelial cells. *Exp Eye Res* **216**:108945, Academic Press.

Dratviman O, Avisar I, Kremer I, Weinberger D, and Goldenberg-Cohen N (2008) Ranibizumab vs. Bevacizumab Treatment of Corneal Neovascularization in Mice. *Invest Ophthalmol Vis Sci* **49**:1474–1474, The Association for Research in Vision and Ophthalmology.

Du J, Zeng C, Li Q, Chen B, Liu H, Huang X, and Huang Q (2012) LPS and TNF-α induce expression of sphingosine-1-phosphate receptor-2 in human microvascular endothelial cells. *Pathol - Res Pract* **208**:82–88, Urban & Fischer.

Eken A, Yetkin MF, Vural A, Okus FZ, Erdem S, Azizoglu ZB, Haliloglu Y, Cakir M, Turkoglu EM, Kilic O, Kara I, Altuntaş HD, Oukka M, Kutuk MS, Mirza M, and Canatan H (2019) Fingolimod alters tissue distribution and cytokine production of human and murine innate lymphoid cells. *Front Immunol* **10**:217, Frontiers Media S.A.

Ensari Delioğlu EN, Uğurlu N, Erdal E, Malekghasemi S, and Çağıl N (2021) Evaluation of sphingolipid metabolism on diabetic retinopathy. *Indian J Ophthalmol* **69**:3376, Wolters Kluwer -- Medknow Publications.

Eresch J, Stumpf M, Koch A, Vutukuri R, Ferreirós N, Schreiber Y, Schröder K, Devraj K, Popp R, Hattenbach LO, Pfeilschifter J, and Pfeilschifter W (2018) Sphingosine Kinase

Downloaded from jpet.aspetjournals.org at ASPET Journals on June 6, 2023

JPET Fast Forward. Published on May 15, 2023 as DOI: 10.1124/jpet.122.001529
This article has not been copyedited and formatted. The final version may differ from this version.

2 Modulates Retinal Neovascularization in the Mouse Model of Oxygen-Induced Retinopathy. *Invest Ophthalmol Vis Sci* **59**:653–661, The Association for Research in Vision and Ophthalmology.

Eski MT, Teberik K, Oltulu P, Ankaralı H, Kaya M, and Alpay M (2022) The effects of subconjunctival bevacizumab, ranibizumab, and aflibercept on corneal neovascularization: *https://doi.org/101177/09603271221084674* **41**:1–11, SAGE PublicationsSage UK: London, England.

Fujii Y, Ueda Y, Ohtake H, Ono N, Takayama T, Nakazawa K, Igarashi Y, and Goitsuka R (2012) Blocking S1P interaction with S1P1 receptor by a novel competitive S1P1-selective antagonist inhibits angiogenesis. *Biochem Biophys Res Commun* **419**:754–760, Academic Press.

Fujita T, Yamabe H, Shimada M, Murakami R, Kumasaka R, Nakamura N, Osawa H, and Okumura K (2008) Thrombin enhances the production of monocyte chemoattractant protein-1 and macrophage inflammatory protein-2 in cultured rat glomerular epithelial cells. *Nephrol Dial Transplant* **23**:3412–3417, Oxford Academic.

Gan L, Fagerholm P, and Palmblad J (2004) Vascular endothelial growth factor (VEGF) and its receptor VEGFR-2 in the regulation of corneal neovascularization and wound healing. *Acta Ophthalmol Scand* **82**:557–563, John Wiley & Sons, Ltd.

Garcia JGN, Liu F, Verin AD, Birukova A, Dechert MA, Gerthoffer WT, Bamburg JR, and English D (2001) Sphingosine 1-phosphate promotes endothelial cell barrier integrity by Edg-dependent cytoskeletal rearrangement. **108**, American Society for Clinical Investigation.

Gardner TW (1995) Histamine, ZO-1 and increased blood-retinal barrier permeability in diabetic retinopathy. *Trans Am Ophthalmol Soc* **93**:583, American Ophthalmological

Downloaded from jpet.aspetjournals.org at ASPET Journals on June 6, 2023

JPET Fast Forward. Published on May 15, 2023 as DOI: 10.1124/jpet.122.001529
This article has not been copyedited and formatted. The final version may differ from this version.

Society.

Gergely P, Nuesslein-Hildesheim B, Guerini D, Brinkmann V, Traebert M, Bruns C, Pan S, Gray NS, Hinterding K, Cooke NG, Groenewegen A, Vitaliti A, Sing T, Luttringer O, Yang J, Gardin A, Wang N, Crumb WJ, Saltzman M, Rosenberg M, and Wallström E (2012) The selective sphingosine 1-phosphate receptor modulator BAF312 redirects lymphocyte distribution and has species-specific effects on heart rate. *Br J Pharmacol* **167**:1035–1047, Br J Pharmacol.

Germana Sanna M, Liao J, Jo E, Alfonso C, Ahn M-Y, Peterson MS, Webb B, Lefebvre S, Chun J, Gray N, and Rosen H (2004) Sphingosine 1-Phosphate (S1P) Receptor Subtypes S1P 1 and S1P 3 , Respectively, Regulate Lymphocyte Recirculation and Heart Rate*. , doi: 10.1074/jbc.M311743200.

Giacomini C, Ferrari G, Bignami F, and Rama P (2014) Alkali burn versus suture-induced corneal neovascularization in C57BL/6 mice: An overview of two common animal models of corneal neovascularization. *Exp Eye Res* **121**:1–4, Academic Press.

Golding-Ochsenbein AAM, Vidal S, Wilmering Wetter B, Guibourdenche C, Beerli C, Chang L, Leonhard S, Holway N, Seuwen K, Jurisic G, Wetter BW, Guibourdenche C, Beerli C, Chang L, Leonhard S, Holway N, Seuwen K, and Jurisic G (2019) S1P-S1PR1 activity controls VEGF-A signaling during lymphatic vessel development. *bioRxiv* 845396, Cold Spring Harbor Laboratory.

Gong K, Jiao J, Xu C, Dong Y, Li D, He D, Zhao D, Yu J, Sun Y, Zhang W, Bai M, and Duan Y (2021) The targetable nanoparticle BAF312@cRGD-CaP-NP represses tumor growth and angiogenesis by downregulating the S1PR1/P-STAT3/VEGFA axis in triple-negative breast cancer. *J Nanobiotechnology* **19**:1–20, BioMed Central Ltd.

Gonzalez-Cabrera PJ, Jo E, Sanna MG, Brown S, Leaf N, Marsolais D, Schaeffer MT,

Downloaded from jpet.aspetjournals.org at ASPET Journals on June 6, 2023

JPET Fast Forward. Published on May 15, 2023 as DOI: 10.1124/jpet.122.001529
This article has not been copyedited and formatted. The final version may differ from this version.

Chapman J, Cameron M, Guerrero M, Roberts E, and Rosen H (2008) Full pharmacological efficacy of a novel S1P1 agonist that does not require S1P-like head-group interactions. *Mol Pharmacol* **74**:1308, NIH Public Access.

Gore A, Kadar T, Cohen M, Gutman H, Cohen L, Gez R, Dachir S, and Horwitz V (2021) Long-term outcome of aflibercept subconjuctival treatment for chemical induced corneal neovascularization in the rabbit model. *Invest Ophthalmol Vis Sci* **62**:911–911, The Association for Research in Vision and Ophthalmology.

Hudson N, Celkova L, Hopkins A, Greene C, Storti F, Ozaki E, Fahey E, Theodoropoulou S, Kenna PF, Humphries MM, Curtis AM, Demmons E, Browne A, Liddie S, Lawrence MS, Grimm C, Cahill MT, Humphries P, Doyle SL, and Campbell M (2019) Dysregulated claudin-5 cycling in the inner retina causes retinal pigment epithelial cell atrophy. *JCI Insight* **4**, American Society for Clinical Investigation.

Igarashi J, Erwin PA, Dantas AP V., Chen H, and Michel T (2003) VEGF induces S1P1 receptors in endothelial cells: Implications for cross-talk between sphingolipid and growth factor receptors. *Proc Natl Acad Sci U S A* **100**:10664, National Academy of Sciences.

Jeya Paul J, Weigel C, Müller T, Heller R, Spiegel S, and Gräler MH (2020) Inflammatory Conditions Disrupt Constitutive Endothelial Cell Barrier Stabilization by Alleviating Autonomous Secretion of Sphingosine 1-Phosphate. *Cells 2020, Vol 9, Page 928* **9**:928, Multidisciplinary Digital Publishing Institute.

Jonas JB, and Neumaier M (2007) Vascular Endothelial Growth Factor and Basic Fibroblast Growth Factor in Exudative Age-Related Macular Degeneration and Diffuse Diabetic Macular Edema. *Ophthalmic Res* **39**:139–142, Karger Publishers.

Kather JN, and Kroll J (2014) Transgenic Mouse Models of Corneal Neovascularization:

Downloaded from jpet.aspetjournals.org at ASPET Journals on June 6, 2023

JPET Fast Forward. Published on May 15, 2023 as DOI: 10.1124/jpet.122.001529
This article has not been copyedited and formatted. The final version may differ from this version.

New Perspectives for Angiogenesis Research. *Invest Ophthalmol Vis Sci* **55**:7637–7651, The Association for Research in Vision and Ophthalmology.

Kim TIT, Kim SSW, Kim SSW, Kim TIT, and Kim EK (2008) Inhibition of experimental corneal neovascularization by using subconjunctival injection of bevacizumab (Avastin). *Cornea* **27**:349–352.

Kimura T, Watanabe T, Sato K, Kon J, Tomura H, Tamama KI, Kuwabara A, Kanda T, Kobayashi I, Ohta H, UI M, and Okajima F (2000) Sphingosine 1-phosphate stimulates proliferation and migration of human endothelial cells possibly through the lipid receptors, Edg-1 and Edg-3. *Biochem J* **348**.

Ko BY, Kim YS, Baek SG, Lee GW, Kim JM, Jean WS, Lee NS, and Kang J (2013) Inhibition of corneal neovascularization by subconjunctival and topical bevacizumab and sunitinib in a rabbit model. *Cornea* **32**:689–695, Cornea.

Kon CH, Occleston NL, Aylward GW, and Khaw PT (1999) Expression of vitreous cytokines in proliferative vitreoretinopathy: A prospective study. *Investig Ophthalmol Vis Sci* **40**:705–712.

Krock BL, Skuli N, and Simon MC (2011) Hypoxia-Induced Angiogenesis: Good and Evil. *Genes Cancer* **2**:1117, Impact Journals, LLC.

Krump-Konvalinkova V, Yasuda S, Rubic T, Makarova N, Mages J, Erl W, Vosseler C, Kirkpatrick CJ, Tigyi G, and Siess W (2005) Stable knock-down of the sphingosine 1-phosphate receptor S1P1 influences multiple functions of human endothelial cells. *Arterioscler Thromb Vasc Biol* **25**:546–552, Lippincott Williams & Wilkins.

Lamalice L, Le Boeuf F, and Huot J (2007) Endothelial Cell Migration During Angiogenesis. *Circ Res* **100**:782–794, Lippincott Williams & Wilkins.

Downloaded from jpet.aspetjournals.org at ASPET Journals on June 6, 2023

JPET Fast Forward. Published on May 15, 2023 as DOI: 10.1124/jpet.122.001529
This article has not been copyedited and formatted. The final version may differ from this version.

Li JK, Wei F, Jin XH, Dai YM, Cui HS, and Li YM (2015) Changes in vitreous VEGF, bFGF and fibrosis in proliferative diabetic retinopathy after intravitreal bevacizumab. *Int J Ophthalmol* **8**:1202, Press of International Journal of Ophthalmology.

Lledó Riquelme M, Campos-Mollo E, and Fernández-Sánchez L (2018) Topical axitinib is a potent inhibitor of corneal neovascularization. *Clin Experiment Ophthalmol* **46**:1063–1074, John Wiley & Sons, Ltd.

Lotery A, Griner R, Ferreira A, Milnes F, and Dugel P (2017) Real-world visual acuity outcomes between ranibizumab and aflibercept in treatment of neovascular AMD in a large US data set. *Eye (Lond)* **31**:1697–1706, Eye (Lond).

Maines LW, French KJ, Wolpert EB, Antonetti DA, and Smith CD (2006a) Pharmacologic manipulation of sphingosine kinase in retinal endothelial cells: Implications for angiogenic ocular diseases. *Invest Ophthalmol Vis Sci* **47**:5022, NIH Public Access.

Maines LW, French KJ, Wolpert EB, Antonetti DA, and Smith CD (2006b) Pharmacologic Manipulation of Sphingosine Kinase in Retinal Endothelial Cells: Implications for Angiogenic Ocular Diseases. *Invest Ophthalmol Vis Sci* **47**:5022–5031, The Association for Research in Vision and Ophthalmology.

McGuire PG, Rangasamy S, Maestas J, and Das A (2011) Pericyte-derived sphinogosine 1-phosphate induces the expression of adhesion proteins and modulates the retinal endothelial cell barrier. *Arterioscler Thromb Vasc Biol* **31**, Lippincott Williams & WilkinsHagerstown, MD.

Mullershausen F, Zecri F, Cetin C, Billich A, Guerini D, and Seuwen K (2009) Persistent signaling induced by FTY720-phosphate is mediated by internalized S1P1 receptors. **5**:428–434.

Downloaded from jpet.aspetjournals.org at ASPET Journals on June 6, 2023

JPET Fast Forward. Published on May 15, 2023 as DOI: 10.1124/jpet.122.001529
This article has not been copyedited and formatted. The final version may differ from this version.

Naito H, Iba T, and Takakura N (2020) Mechanisms of new blood-vessel formation and proliferative heterogeneity of endothelial cells. *Int Immunol* **32**:295–305, Oxford Academic.

Nakamura S, Imai S, Ogishima H, Tsuruma K, Shimazawa M, and Hara H (2012) Morphological and Functional Changes in the Retina after Chronic Oxygen-Induced Retinopathy. *PLoS One* **7**:e32167, Public Library of Science.

Nishihara H, Shimizu F, Sano Y, Takeshita Y, Maeda T, Abe M, Koga M, and Kanda T (2015) Fingolimod Prevents Blood-Brain Barrier Disruption Induced by the Sera from Patients with Multiple Sclerosis. *PLoS One* **10**, PLOS.

O'Sullivan C, and Dev KK (2013) The structure and function of the S1P1 receptor. *Trends Pharmacol Sci* **34**:401–412, Elsevier Current Trends.

Paik JH, Chae SS, Lee MJ, Thangada S, and Hla T (2001) Sphingosine 1-Phosphate-induced Endothelial Cell Migration Requires the Expression of EDG-1 and EDG-3 Receptors and Rho-dependent Activation of αvβ3- and β1-containing Integrins. *J Biol Chem* **276**:11830–11837, Elsevier.

Park YR, and Chung SK (2015) Inhibitory Effect of Topical Aflibercept on Corneal Neovascularization in Rabbits. *Cornea* **34**:1303–1307, Lippincott Williams and Wilkins.

Percie du Sert N, Hurst V, Ahluwalia A, Alam S, Avey MT, Baker M, Browne WJ, Clark A, Cuthill IC, Dirnagl U, Emerson M, Garner P, Holgate ST, Howells DW, Karp NA, Lazic SE, Lidster K, MacCallum CJ, Macleod M, Pearl EJ, Petersen OH, Rawle F, Reynolds P, Rooney K, Sena ES, Silberberg SD, Steckler T, and Würbel H (2020) The ARRIVE guidelines 2.0: Updated guidelines for reporting animal research*. *J Cereb Blood Flow Metab* **40**:1769–1777, SAGE Publications Ltd.

Downloaded from jpet.aspetjournals.org at ASPET Journals on June 6, 2023

JPET Fast Forward. Published on May 15, 2023 as DOI: 10.1124/jpet.122.001529
This article has not been copyedited and formatted. The final version may differ from this version.

Pognan F, Mahl JA, Papoutsi M, Ledieu D, Raccuglia M, Theil D, Voytek SB, Devine PJ, Kubek-Luck K, Claudio N, Cordier A, Heier A, Kolly C, Hartmann A, Chibout SD, Bouchard P, and Trendelenburg C (2018) Induction of hemangiosarcoma in mice after chronic treatment with S1P-modulator siponimod and its lack of relevance to rat and human. *Arch Toxicol* **92**:1877, Springer.

Porter H, Qi H, Prabhu N, Grambergs R, McRae J, Hopiavuori B, and Mandal N (2018) Characterizing Sphingosine Kinases and Sphingosine 1-Phosphate Receptors in the Mammalian Eye and Retina. *Int J Mol Sci 2018, Vol 19, Page 3885* **19**:3885, Multidisciplinary Digital Publishing Institute.

Proia RL, and Hla T (2015) Emerging biology of sphingosine-1-phosphate: its role in pathogenesis and therapy. *J Clin Invest* **125**:1379, American Society for Clinical Investigation.

Qiu T, Cui L, Xu J-J, Hong J-X, and Xiang J (2020) Reconstruction of the ocular surface by autologous transplantation of rabbit adipose tissue-derived stem cells on amniotic membrane. *Ann Transl Med* **8**:1062–1062, AME Publications.

Rikitake Y, Hirata KI, Kawashima S, Ozaki M, Takahashi T, Ogawa W, Inoue N, and Yokoyama M (2002) Involvement of Endothelial Nitric Oxide in Sphingosine-1-Phosphate–Induced Angiogenesis. *Arterioscler Thromb Vasc Biol* **22**:108–114, Lippincott Williams & Wilkins.

Salomone S, and Waeber C (2011) Selectivity and specificity of sphingosine-1-phosphate receptor ligands: Caveats and critical thinking in characterizing receptor-mediated effects. *Front Pharmacol* **FEB**, Front Pharmacol.

Sartawi Z, Ryan KB, and Waeber C (2020) Bone regenerative potential of the selective sphingosine 1-phosphate receptor modulator siponimod: In vitro characterisation using

Downloaded from jpet.aspetjournals.org at ASPET Journals on June 6, 2023

JPET Fast Forward. Published on May 15, 2023 as DOI: 10.1124/jpet.122.001529
This article has not been copyedited and formatted. The final version may differ from this version.

osteoblast and endothelial cells. *Eur J Pharmacol* **882**:173262, Elsevier.

Schmid G, Guba M, Ischenko I, Papyan A, Joka M, Schrepfer S, Bruns CJ, Jauch KW, Heeschen C, and Graeb C (2007) The immunosuppressant FTY720 inhibits tumor angiogenesis via the sphingosine 1-phosphate receptor 1. *J Cell Biochem* **101**:259–270, John Wiley & Sons, Ltd.

Schuhmann MK, Bittner S, Meuth SG, Kleinschnitz C, and Fluri F (2015) Fingolimod (FTY720-P) Does Not Stabilize the Blood–Brain Barrier under Inflammatory Conditions in an in Vitro Model. *Int J Mol Sci 2015, Vol 16, Pages 29454-29466* **16**:29454–29466, Multidisciplinary Digital Publishing Institute.

Scott LJ (2020) Siponimod: A Review in Secondary Progressive Multiple Sclerosis. *CNS Drugs* **34**:1191–1200, Adis.

Shu X, Wu W, Mosteller RD, and Broek D (2002) Sphingosine Kinase Mediates Vascular Endothelial Growth Factor-Induced Activation of Ras and Mitogen-Activated Protein Kinases. *Mol Cell Biol* **22**:7758, Taylor & Francis.

Soleimani R, Heytens E, and Oktay K (2011) Enhancement of Neoangiogenesis and Follicle Survival by Sphingosine-1-Phosphate in Human Ovarian Tissue Xenotransplants. *PLoS One* **6**:e19475, Public Library of Science.

Spampinato SF, Costantino G, Merlo S, Canonico PL, and Sortino MA (2022) Microglia Contributes to BAF-312 Effects on Blood–Brain Barrier Stability. *Biomolecules* **12**, Multidisciplinary Digital Publishing Institute (MDPI).

Spampinato SF, Merlo S, Sano Y, Kanda T, and Sortino MA (2021) Protective effect of the sphingosine-1 phosphate receptor agonist siponimod on disrupted blood brain barrier function. *Biochem Pharmacol* **186**:114465, Elsevier.

Downloaded from jpet.aspetjournals.org at ASPET Journals on June 6, 2023

JPET Fast Forward. Published on May 15, 2023 as DOI: 10.1124/jpet.122.001529
This article has not been copyedited and formatted. The final version may differ from this version.

Spranger J, Meyer-Schwickerath R, Klein M, Schatz H, and Pfeiffe A (1995) TNF-alpha level in the vitreous body. Increase in neovascular eye diseases and proliferative diabetic retinopathy.

Srinivasan B, Kolli AR, Esch MB, Abaci HE, Shuler ML, and Hickman JJ (2015) TEER measurement techniques for in vitro barrier model systems. *J Lab Autom* **20**:107, NIH Public Access.

Suarez S, McCollum GW, Bretz CA, Yang R, Capozzi ME, and Penn JS (2014) Modulation of VEGF-Induced Retinal Vascular Permeability by Peroxisome Proliferator-Activated Receptor-β/δ. *Invest Ophthalmol Vis Sci* **55**:8232, Association for Research in Vision and Ophthalmology.

Suzuki Y, Nakazawa M, Suzuki K, Yamazaki H, and Miyagawa Y (2011) Expression profiles of cytokines and chemokines in vitreous fluid in diabetic retinopathy and central retinal vein occlusion. *Jpn J Ophthalmol* **55**:256–263, Jpn J Ophthalmol.

Swan DJ, Kirby JA, and Ali S (2010) Vascular biology: the role of sphingosine 1-phosphate in both the resting state and inflammation. *J Cell Mol Med* **14**:2211, Wiley-Blackwell.

Takabe K, Paugh SW, Milstien S, and Spiegel S (2008) "Inside-out" signaling of sphingosine-1-phosphate: therapeutic targets. *Pharmacol Rev* **60**:181–195, Pharmacol Rev.

Tarrasón G, Aulí M, Mustafa S, Dolgachev V, Domènech MT, Prats N, Domínguez M, López R, Aguilar N, Calbet M, Pont M, Milligan G, Kunkel SL, and Godessart N (2011) The sphingosine-1-phosphate receptor-1 antagonist, W146, causes early and short-lasting peripheral blood lymphopenia in mice. *Int Immunopharmacol* **11**:1773–1779, Elsevier.

Downloaded from jpet.aspetjournals.org at ASPET Journals on June 6, 2023

JPET Fast Forward. Published on May 15, 2023 as DOI: 10.1124/jpet.122.001529
This article has not been copyedited and formatted. The final version may differ from this version.

Terao R, Honjo M, Ueta T, Obinata H, Izumi T, Kurano M, Yatomi Y, Koso H, Watanabe S, and Aihara M (2019) Light Stress-Induced Increase of Sphingosine 1-Phosphate in Photoreceptors and Its Relevance to Retinal Degeneration. *Int J Mol Sci 2019, Vol 20, Page 3670* **20**:3670, Multidisciplinary Digital Publishing Institute.

Ucgul RK, Celebi S, Yilmaz NS, Bukan N, and Ucgul AY (2021) Intrastromal versus subconjunctival anti-VEGF agents for treatment of corneal neovascularization: a rabbit study. *Eye 2021 3511* **35**:3123–3130, Nature Publishing Group.

Wallsh JO, and Gallemore RP (2021) Anti-VEGF-Resistant Retinal Diseases: A Review of the Latest Treatment Options. *Cells* **10**, Multidisciplinary Digital Publishing Institute (MDPI).

Wang J, Chen S, Jiang F, You C, Mao C, Yu J, Han J, Zhang Z, and Yan H (2014) Vitreous and Plasma VEGF Levels as Predictive Factors in the Progression of Proliferative Diabetic Retinopathy after Vitrectomy. *PLoS One* **9**:e110531, Public Library of Science.

Wilkerson BA, and Argraves KM (2014) The role of sphingosine-1-phosphate in endothelial barrier function. *Biochim Biophys Acta* **1841**:1403, NIH Public Access.

Xiong Y, and Hla T (2014) S1P Control of Endothelial Integrity. *Curr Top Microbiol Immunol* **378**:85, NIH Public Access.

Xu CB, Zhang Y, Stenman E, and Edvinsson L (2002) d-erythro-N,N-dimethylsphingosine inhibits bFGF-induced proliferation of cerebral, aortic and coronary smooth muscle cells. *Atherosclerosis* **164**:237–243, Elsevier.

Yanagida K, Liu CH, Faraco G, Galvani S, Smith HK, Burg N, Anrather J, Sanchez T, Iadecola C, and Hla T (2017) Size-selective opening of the blood-brain barrier by targeting endothelial sphingosine 1-phosphate receptor 1. *Proc Natl Acad Sci U S A*

Downloaded from jpet.aspetjournals.org at ASPET Journals on June 6, 2023

JPET Fast Forward. Published on May 15, 2023 as DOI: 10.1124/jpet.122.001529
This article has not been copyedited and formatted. The final version may differ from this version.

114:4531–4536, National Academy of Sciences.

Zhang Y, Han Y, Zhao Y, Lv Y, Hu Y, Tan Y, Bi X, Yu B, and Kou J (2017) DT-13 ameliorates TNF-α-Induced vascular endothelial hyperpermeability via non-muscle myosin IIA and the Src/PI3K/Akt signaling pathway. *Front Immunol* **8**:925, Frontiers Media S.A.

Zheng Z, Zeng Y, Zhu X, Tan Y, Li Y, Li Q, and Yi G (2019) ApoM-S1P Modulates Ox-LDL-Induced Inflammation Through the PI3K/Akt Signaling Pathway in HUVECs. *Inflammation* **42**:606–617, Springer New York LLC.

Zou Y, Hu J, Huang W, Ye S, Han F, Du J, Shao M, Guo R, Lin J, Zhao Y, Xiong Y, and Wang X (2020) Non-Mitogenic Fibroblast Growth Factor 1 Enhanced Angiogenesis Following Ischemic Stroke by Regulating the Sphingosine-1-Phosphate 1 Pathway. *Front Pharmacol* **11**:59, Frontiers Media S.A.

Downloaded from jpet.aspetjournals.org at ASPET Journals on June 6, 2023

JPET Fast Forward. Published on May 15, 2023 as DOI: 10.1124/jpet.122.001529
This article has not been copyedited and formatted. The final version may differ from this version.

Figures legends

Fig. 1. Effects of siponimod and W146 on endothelial cells metabolic activity measured by MTT. Cells were incubated for 48 hours in CGM with the indicated concentration of siponimod (A: HUVEC; C: HRMEC) or W146 (B: HUVEC; D: HRMEC). Data are expressed as a percentage of the control metabolic activity (CGM; complete growth medium) which was set to 100% in each replicate. Bars are showing the mean, error bars represent the standard deviation, and the black circles represent the values of independent replicates ($n \geq 4$). Statistical analysis was carried out on the raw absorbance data using randomized complete block ANOVA. Tukey's multiple comparisons was employed as a post hoc test only when the ANOVA yielded a p-value less than 0.05. *: $p < 0.05$, **: $p < 0.01$, ***: $p < 0.001$.

Fig. 2. Effects of siponimod and W146 on lactate dehydrogenase (LDH) release from endothelial cells. Cells were incubated for 48 hours in CGM with the indicated concentration of siponimod (A: HUVEC; C: HRMEC) or W146 (B: HUVEC; D: HRMEC). Data are expressed as percent cytotoxicity, with bars showing the mean, error bars representing the standard deviation, and black circles representing the values of independent replicates ($n \geq 3$). Statistical analysis was carried using randomized complete block ANOVA. Tukey's multiple comparisons was employed as a post hoc test only when the ANOVA yielded a p-value less than 0.05. *: $p < 0.05$, **: $p < 0.01$, ***: $p < 0.001$.

Fig. 3. Effect of siponimod (A and C) and W146 (B and D) on endothelial cell proliferation assessed using BrdU incorporation assay. HUVEC (A and B) or HRMEC (C and D) were incubated for 48 hours with the selected drug in reduced growth medium (RGM) before adding BrdU. The BrdU incorporation was assayed by measuring absorbance at 405 nm.

Downloaded from jpet.aspetjournals.org at ASPET Journals on June 6, 2023

JPET Fast Forward. Published on May 15, 2023 as DOI: 10.1124/jpet.122.001529
This article has not been copyedited and formatted. The final version may differ from this version.

Absorbance of endothelial cells incubated in complete growth medium (CGM; positive control) was set to 100% in each replicate and the data is expressed as a percentage of the control absorbance. The bars, error bars, and black circles represent the mean, standard deviation, and values of independent replicates ($n \geq 4$). Statistical comparisons were carried out on the raw absorbance values of treated cells using randomized complete block ANOVA. Tukey's multiple comparison was employed as a post hoc test only when the ANOVA yielded a p-value less than 0.05. ***: $p < 0.001$.

Fig. 4. Effect of siponimod (sipo) and W146 on bFGF-induced endothelial cell proliferation assessed using BrdU incorporation assay (A and B: HUVEC; C and D: HRMEC). Cells were incubated for 72 hours with or without bFGF (25 ng/ml) and the indicated drug concentration before adding BrdU for 6 hours. The absorbance of endothelial cells incubated in the carrier medium (basal medium supplemented with 1% FBS, 2 mg/ml hydrocortisone; negative control) was set to 100% in each replicate and the data is expressed as a percentage of the control absorbance. The bars, error bars, and black circles represent the mean, standard deviation, and values of independent replicates, respectively. Statistical comparisons were carried out on the raw absorbance values of treated cells using randomized complete block ANOVA. Tukey's multiple comparison was employed as a post hoc test only when the ANOVA yielded a p-value less than 0.05. *: $p < 0.05$, **: $p < 0.01$, ***: $p < 0.001$. NS: $p > 0.05$.

Fig. 5. Effect of siponimod and W146 on VEGF-induced endothelial cell proliferation using the BrdU incorporation assay. Panels A and B show the results in HUVEC and panels C and D show the results in HRMEC. Endothelial cells were incubated for 72 hours with or without VEGF (40 ng/ml) and the selected drug concentration before adding BrdU for 6 hours. The

Downloaded from jpet.aspetjournals.org at ASPET Journals on June 6, 2023

JPET Fast Forward. Published on May 15, 2023 as DOI: 10.1124/jpet.122.001529
This article has not been copyedited and formatted. The final version may differ from this version.

absorbance of endothelial cells incubated in the carrier medium (basal medium supplemented with 1% FBS, 2 mg/ml hydrocortisone; negative control) was set to 100% in each replicate and the data is expressed as a percentage of the control absorbance. The bars, error bars, and black circles represent the mean, standard deviation, and values of independent replicates, respectively. Statistical comparisons were carried out on the raw absorbance values of treated cells using randomized complete block ANOVA. Tukey's multiple comparison was employed as a post-hoc test only when the ANOVA yielded a p-value less than 0.05. *: $p < 0.05$, **: $p < 0.01$, ***: $p < 0.001$. NS: $p > 0.05$.

Fig. 6. Effect of siponimod and W146 on endothelial cell migration towards high chemoattractant concentration. The tested chemoattractants include 10% FBS (HUVEC migration is shown in panels A, B, C, and HRMEC migration is shown in panels D, E, F: HRMEC), 3 μM S1P (HRMEC migration in panel G), and 40 ng/ml VEGF (HRMEC migration in panel H). Cells in the top chamber were allowed to migrate towards 10% FBS, S1P in RGM or VEGF in RGM in the bottom chamber in the presence of the drug concentration indicated (siponimod or W146 in both the top and bottom chambers). Cell count on the bottom side of the membrane (migrating cells) towards 10% FBS only (positive control) was set to 100% in each replicate, and cell count in each treatment group was expressed as a percent of the control. (A) and (B) show the relative HUVEC count on the bottom side of the membrane in presence of increasing siponimod and W146 concentrations, respectively. (C) shows representative images for the bottom side of the transwell membrane in 10% FBS and RGM in the top panels and 100 nM siponimod and 10 μM W146 in the bottom panels. (D) and (E) show the relative HRMEC count on the bottom side of the

Downloaded from jpet.aspetjournals.org at ASPET Journals on June 6, 2023

JPET Fast Forward. Published on May 15, 2023 as DOI: 10.1124/jpet.122.001529
This article has not been copyedited and formatted. The final version may differ from this version.

membrane in the presence of increasing siponimod and W146 concentrations, respectively. (F) shows representative images for the bottom side of the transwell membrane in 10% FBS and RGM in the top panels and 100 nM siponimod and 10 μM W146 in the bottom panels. G shows the relative HRMEC count on the bottom side of the membrane in the presence of S1P (3μM) with or without siponimod (100 nM) or W146 (10 μM). H shows the relative HRMEC count on the bottom side of the membrane in the presence of VEGF (40 ng/ml) with or without siponimod (100 nM) or W146 (10 μM). I shows representative images for the bottom side of the transwell membrane in 3μM S1P (top left panel), 40 ng/ml VEGF (top right panel), 3 μM S1P with 100 nM siponimod (middle left panel), and 40 ng/ml VEGF with 100 nM siponimod (middle right panel), 3μM S1P with 10 μM W146 (bottom left panel) and 40 ng/ml VEGF with 10 μM W146 (bottom right panel). The bars, error bars, and black circles represent the mean, standard deviation, and values of independent replicates, respectively. Statistical comparisons were carried out on the raw cell count values using randomized complete block ANOVA. Tukey's multiple comparison was employed as a post hoc test only when the ANOVA yielded a p-value less than 0.05. *: $p < 0.05$, **: $p < 0.01$, ***: $p < 0.001$.

Fig. 7. Effects of siponimod and W146 on HRMEC barrier function measured by TEER (A and C) and FITC-DEX permeability (B and D). A and B: HRMEC barrier function was first assessed under basal conditions to monitor the effect of siponimod and W146 on resting barrier permeability. In a second set of experiments (C and D), the endothelial barrier was challenged with 50 ng/ml TNF-α applied at time zero, with or without siponimod (100 nM) or W146 (10 μM). TEER was measured at 0 (immediately before drug application), 24, and 48 hours (A and C). FITC-DEX permeability was measured at 48 hours (B and D). Statistical comparisons were carried out on the raw TEER values and apparent permeability coefficient

Downloaded from jpet.aspetjournals.org at ASPET Journals on June 6, 2023

JPET Fast Forward. Published on May 15, 2023 as DOI: 10.1124/jpet.122.001529
This article has not been copyedited and formatted. The final version may differ from this version.

values using randomized complete block ANOVA ($n \geq 5$). Tukey's multiple comparison was employed as a post hoc test only when the ANOVA yielded a p-value less than 0.05. *: $p < 0.05$, **: $p < 0.01$, ***: $p < 0.001$. NS: $p > 0.05$.

Fig. 8. Effect of **s**iponimod on endothelial junction protein expression and localization in HRMEC. A shows the average score of claudin distribution in retinal endothelial cells when incubated under control complete growth medium conditions (CGM) or TNF-α (25 ng/ml) with or without 100 nM siponimod (Sipo 100 nM) or 10 μM W146. B shows the average score of ZO-1 distribution in retinal endothelial cells when incubated under control complete growth medium conditions (CGM) or TNF-α (25 ng/ml) with or without 100 nM siponimod (Sipo 100 nM) or 10 μM W146. C shows the average score of VE-cadherin distribution in retinal endothelial cells when incubated under control complete growth medium conditions (CGM) or TNF-α (25 ng/ml) with or without 100 nM siponimod (Sipo 100 nM) or 10 μM W146. The endothelial junction protein distribution in each image was scored according to three features (continuity of protein staining in the intercellular junction, the intensity of staining in the intercellular junction, and overall presence of the protein in the intercellular junction). For each feature, the image was scored by an investigator blinded to the treatment group from 0-4 with 4 being the maximum property. At least three random images were taken and ranked for each coverslip, and at least two coverslips per group were employed in independent replicate. Each experiment was performed independently at least 5 times (n =5). Data were analyzed using the Kruskal-Wallis test followed by Dunn's multiple comparison post-hoc test as the Kruskal-Wallis test yielded a p-value of 0.002. D shows representative images for claudin-5, ZO-1, and VE-cadherin staining in HRMEC when incubated under control CGM, TNF- α (25 ng/ml), siponimod (100 nM) with TNF- α and W146 (10 mM)

Downloaded from jpet.aspetjournals.org at ASPET Journals on June 6, 2023

JPET Fast Forward. Published on May 15, 2023 as DOI: 10.1124/jpet.122.001529
This article has not been copyedited and formatted. The final version may differ from this version.

with TNF- α (from top to bottom). The experimental conditions were applied for 6 hours before the cells were fixed and stained. Single-head arrows indicate the formation of uninterrupted lines of staining in the intercellular boundaries and double-head arrows indicated interrupted non-continuous stained lines.

Fig. 9. Siponimod inhibits the progression of neovascularization in suture-induced corneal neovascularization in albino rabbits. Panel (A) shows a timeline of the experiment. Panel (B) shows the neovascular area at time zero (before administration of the first dose on day 15) and day 9 (72 hours after administration of the third dose on day 23). Panel (C) shows representative images from each treatment group. Statistical comparisons were carried out using repeated measures ANOVA (n =12). The animal received three subconjunctival injections (100 µl each) of a stock siponimod concentration of 5.16 µg/ml and 40 µg/ml for low dose siponimod (Low dose sipo) and high dose siponimod (High dose sipo), respectively. Solvent is 0.08% DMSO in PBS which is the solvent base used to dissolve siponimod. Data were analyzed using repeated measures ANOVA (n =12). Tukey's multiple comparison was employed as a post hoc test only when the ANOVA yielded a p-value less than 0.05. *: $p < 0.05$, **: $p < 0.01$, ***: $p < 0.001$. Panel (D) shows representative images for H&E staining of the corneal sections showing the morphological changes (from left to right) in untreated control corneas, solvent, low dose siponimod, and high dose siponimod. The images were taken from the peripheral corneas of seven rabbits in each treatment group (n=7). The images show distorted stroma (indicated by black circles), thinning discontinuous epithelium (indicated by arrows), and increased cellular infiltration (indicated by asterisks).

Downloaded from jpet.aspetjournals.org at ASPET Journals on June 6, 2023

Table 1. Summary of the effects of siponimod and W146 in endothelial cells functional assays using either human umbilical vein endothelial cells (HUVEC) or retinal microvascular endothelial cells (HRMEC).

Endothelial function	Assessment method	Incubation time (hr)[1]	Possible S1P source	Modulator effect[2]			
				HUVEC		HRMEC	
				Siponimod	W-146	Siponimod	W-146
Cell proliferation	BrdU assay	48	Endogenous[3]	No effect	No effect	No effect	No effect
VEGF-induced proliferation	BrdU assay	72	Endogenous	No effect	Decrease	No effect	Decrease
bFGF-induced proliferation	BrdU assay	72	Endogenous	No effect	Decrease	No effect	Decrease
Chemotaxis	Transwell migration toward 10% serum	6	Endogenous and exogenous[4]	Decrease	Decrease	Decrease	Decrease
	Transwell migration toward VEGF (40 ng/ml)	6	Endogenous [4]	-	-	Decrease	Decrease
	Transwell migration toward S1P (3 μM)	6	Endogenous [4]	-	-	Decrease	Decrease
	Transwell migration toward the modulator	6	Endogenous	Increase	No effect	Increase	No effect
Chemokinesis	Wound healing assay	12	Endogenous	Increase	No effect	-	-

Downloaded from jpet.aspetjournals.org at ASPET Journals on June 6, 2023

JPET Fast Forward. Published on May 15, 2023 as DOI: 10.1124/jpet.122.001529
This article has not been copyedited and formatted. The final version may differ from this version.

Resting barrier function	TEER	24 and 48	Endogenous	-	-	Increase	No effect
	FITC-DEX permeability	48	Endogenous	-	-	Decrease permeability	No effect
TNF-α induced barrier disruption	TEER	24 and 48	Endogenous and exogenous	-	-	Increase TEER	No effect
	FITC-DEX permeability	48	Endogenous and exogenous	-	-	Decreased permeability	No effect
TNF-α induced claudin-5 disruption	Immunofluorescence	6	Endogenous and exogenous	-	-	Decreased disruption	No effect
TNF-α induced ZO-1 disruption	Immunofluorescence	6	Endogenous and exogenous	-	-	Decreased disruption	No effect
TNF-α induced VE-cadherin	Immunofluorescence	6	Endogenous and exogenous	-	-	Decreased disruption	No effect

[1] Incubation time is the total time of cell exposure to the modulator. [2] Modulator effect represents the general outcome for each assessment method. [3] Endogenous S1P refers to the experiments where cells were incubated with reduced growth medium or controlled mediums with $\leq$ 2% FBS and in which the only S1P present was that presumably synthesized by endothelial cells. [4] Exogenous S1P refers to the experiments where the cells were incubated with complete growth medium or complete growth medium with additional 10% FBS.

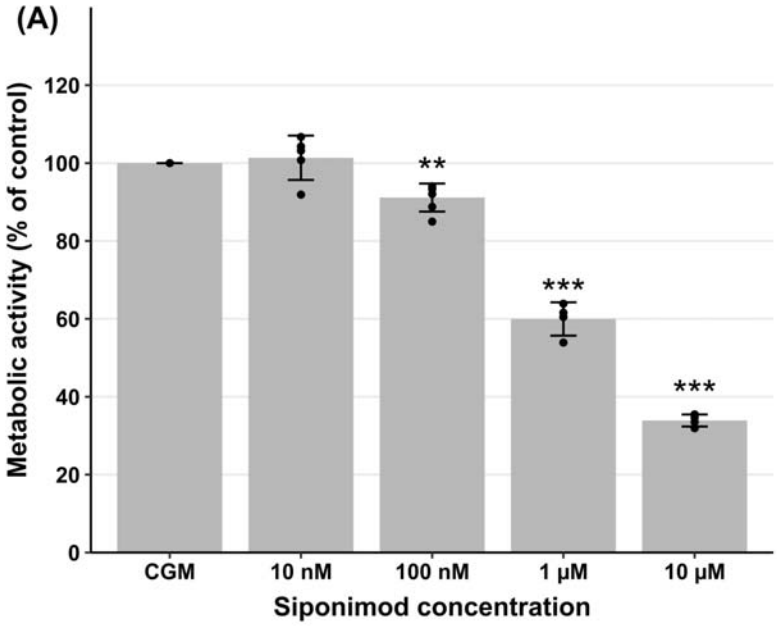
Downloaded from jpet.aspetjournals.org at ASPET Journals on June 6, 2023

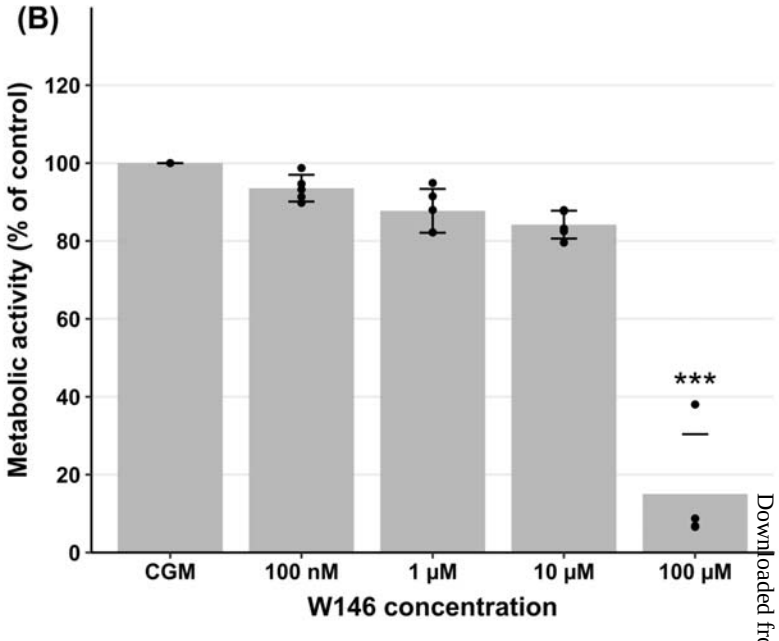
JPET Fast Forward. Published on May 15, 2023 as DOI: 10.1124/jpet.122.001529
This article has not been copyedited and formatted. The final version may differ from this version.

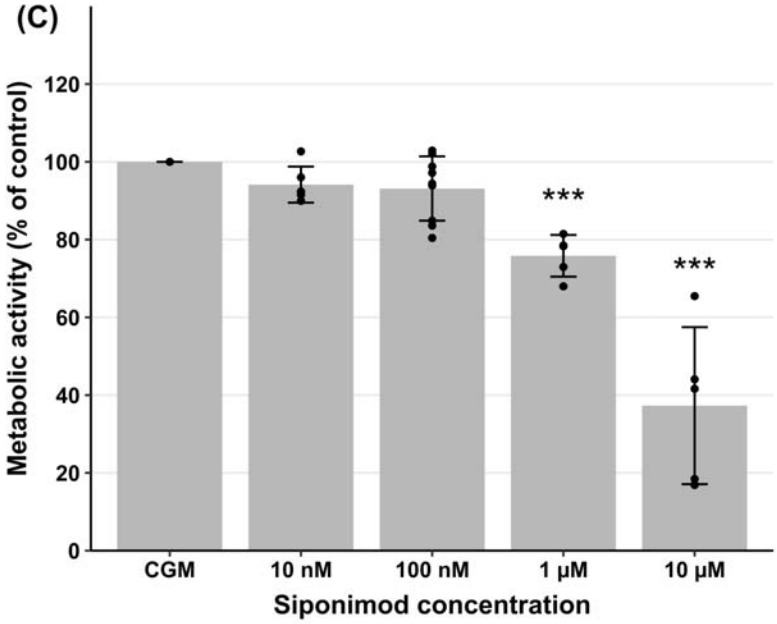
Downloaded from jpet.aspetjournals.org at ASPET Journals on June 6, 2023

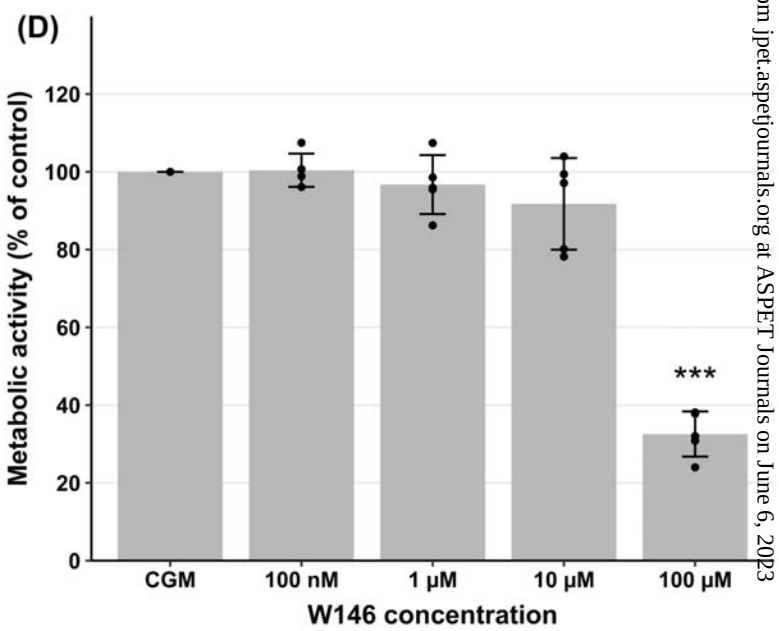
JPET Fast Forward. Published on May 15, 2023 as DOI: 10.1124/jpet.122.001529
This article has not been copyedited and formatted. The final version may differ from this version.

JPET Fast Forward. Published on May 15, 2023 as DOI: 10.1124/jpet.122.001529
This article has not been copyedited and formatted. The final version may differ from this version.





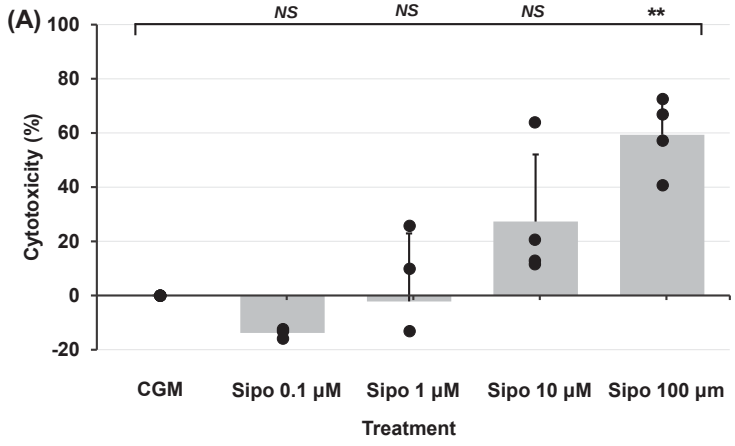


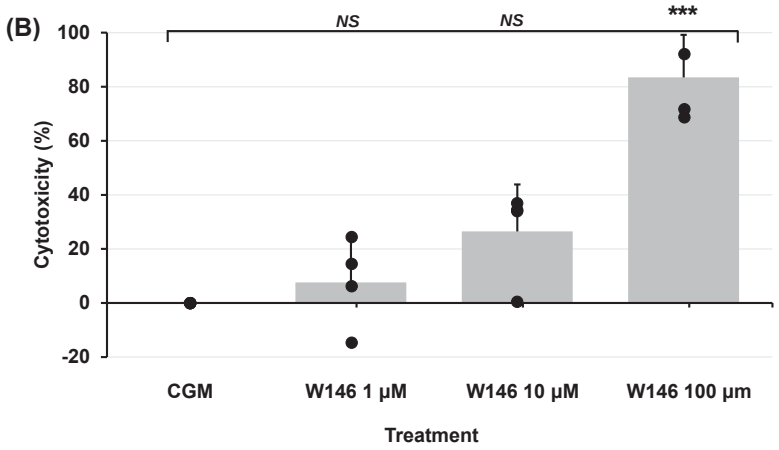


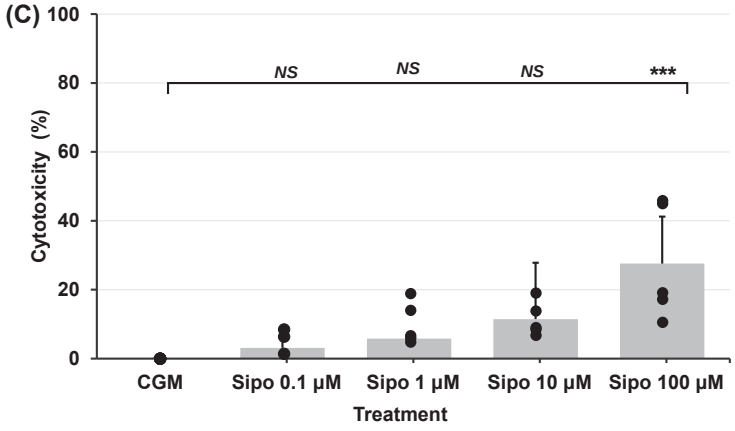
Downloaded from jpet.aspetjournals.org at ASPET Journals on June 6, 2023

Fig. 1

JPET Fast Forward. Published on May 15, 2023 as DOI: 10.1124/jpet.122.001529
This article has not been copyedited and formatted. The final version may differ from this version.







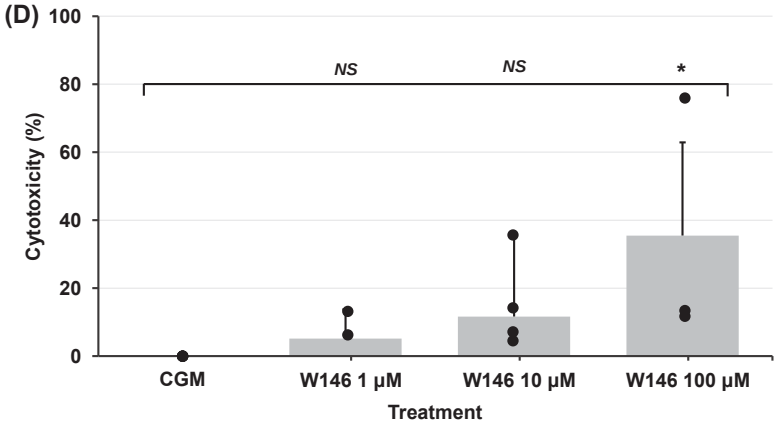


Fig.2

Downloaded from jpet.aspetjournals.org at ASPET Journals on June 6, 2023

JPET Fast Forward. Published on May 15, 2023 as DOI: 10.1124/jpet.122.001529
This article has not been copyedited and formatted. The final version may differ from this version.

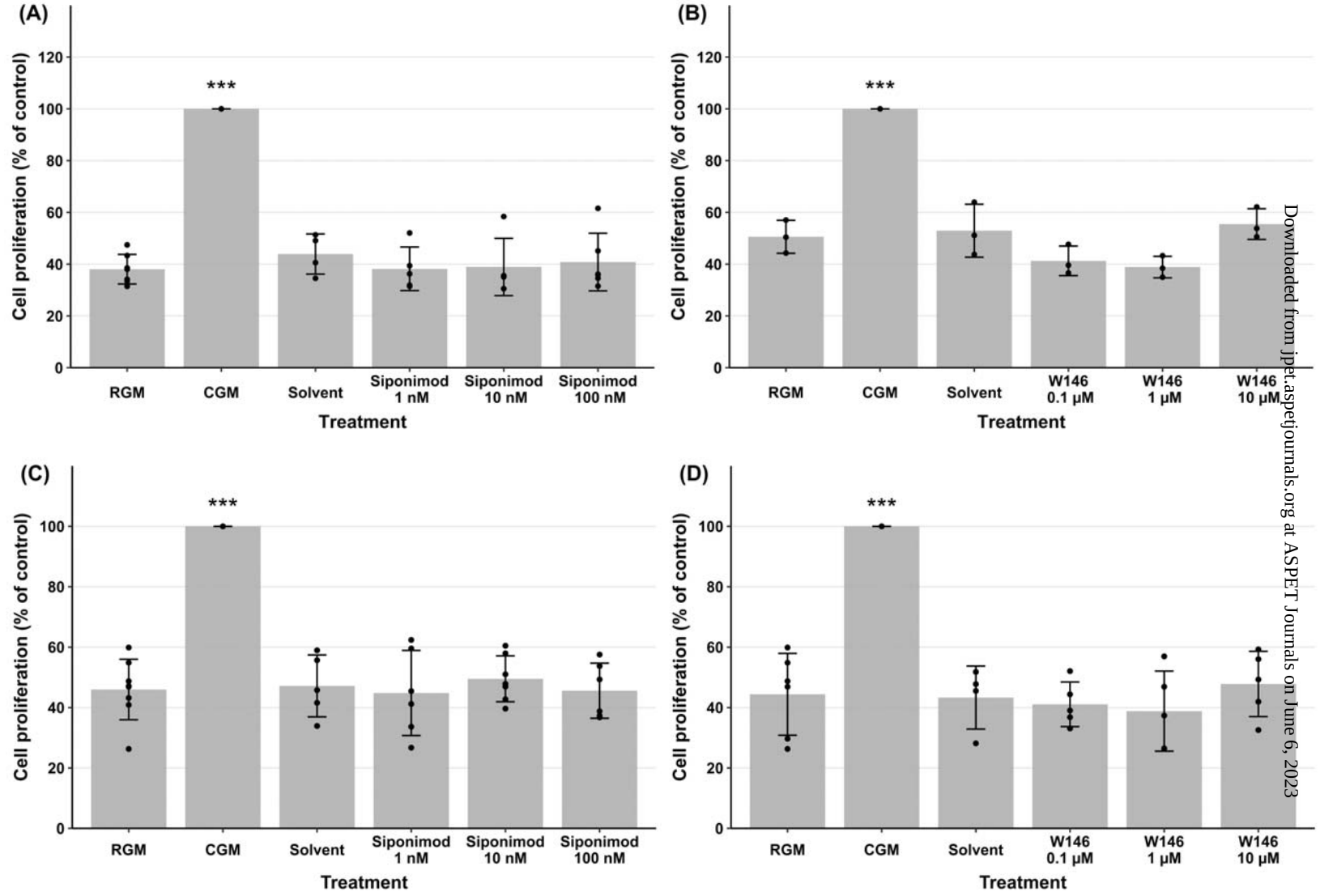
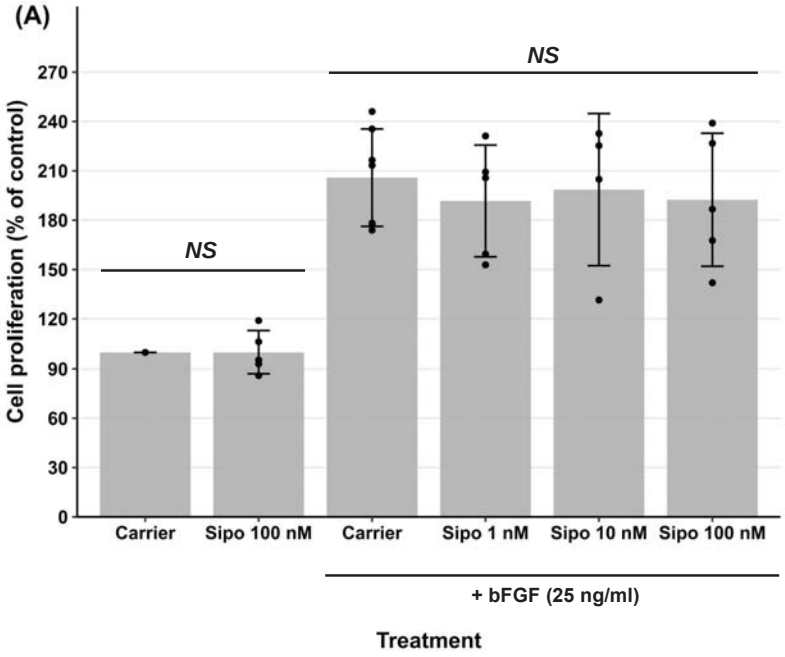
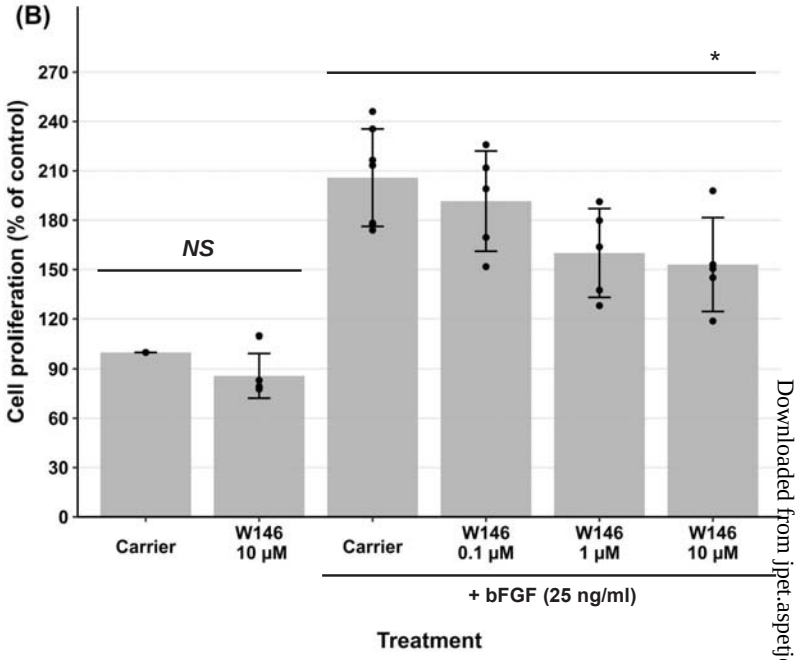


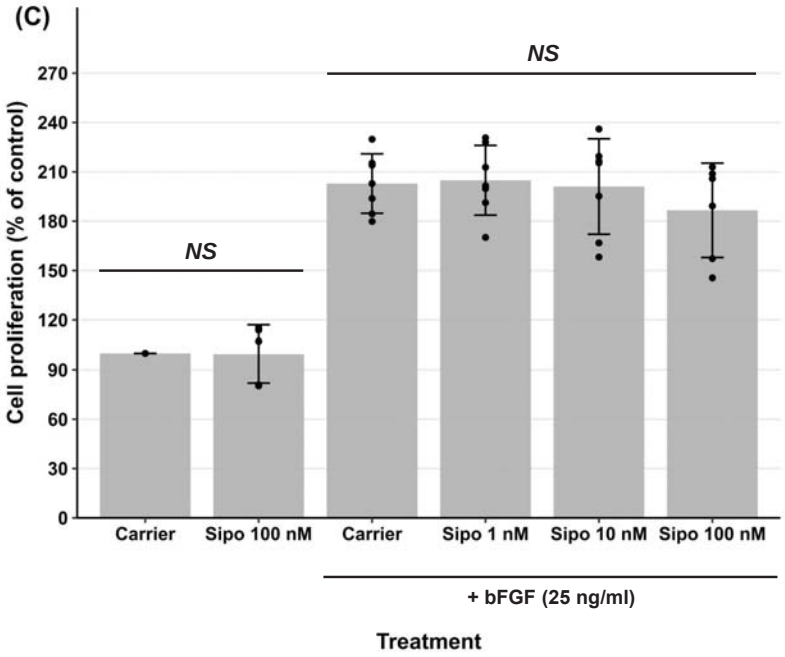
Fig. 3

Downloaded from jpet.aspetjournals.org at ASPET Journals on June 6, 2023

JPET Fast Forward. Published on May 15, 2023 as DOI: 10.1124/jpet.122.001529
This article has not been copyedited and formatted. The final version may differ from this version.







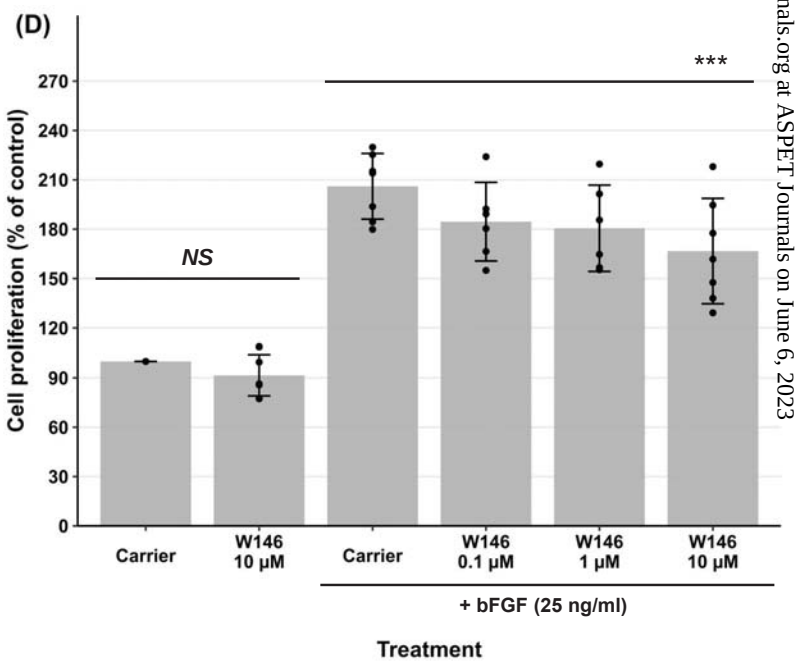
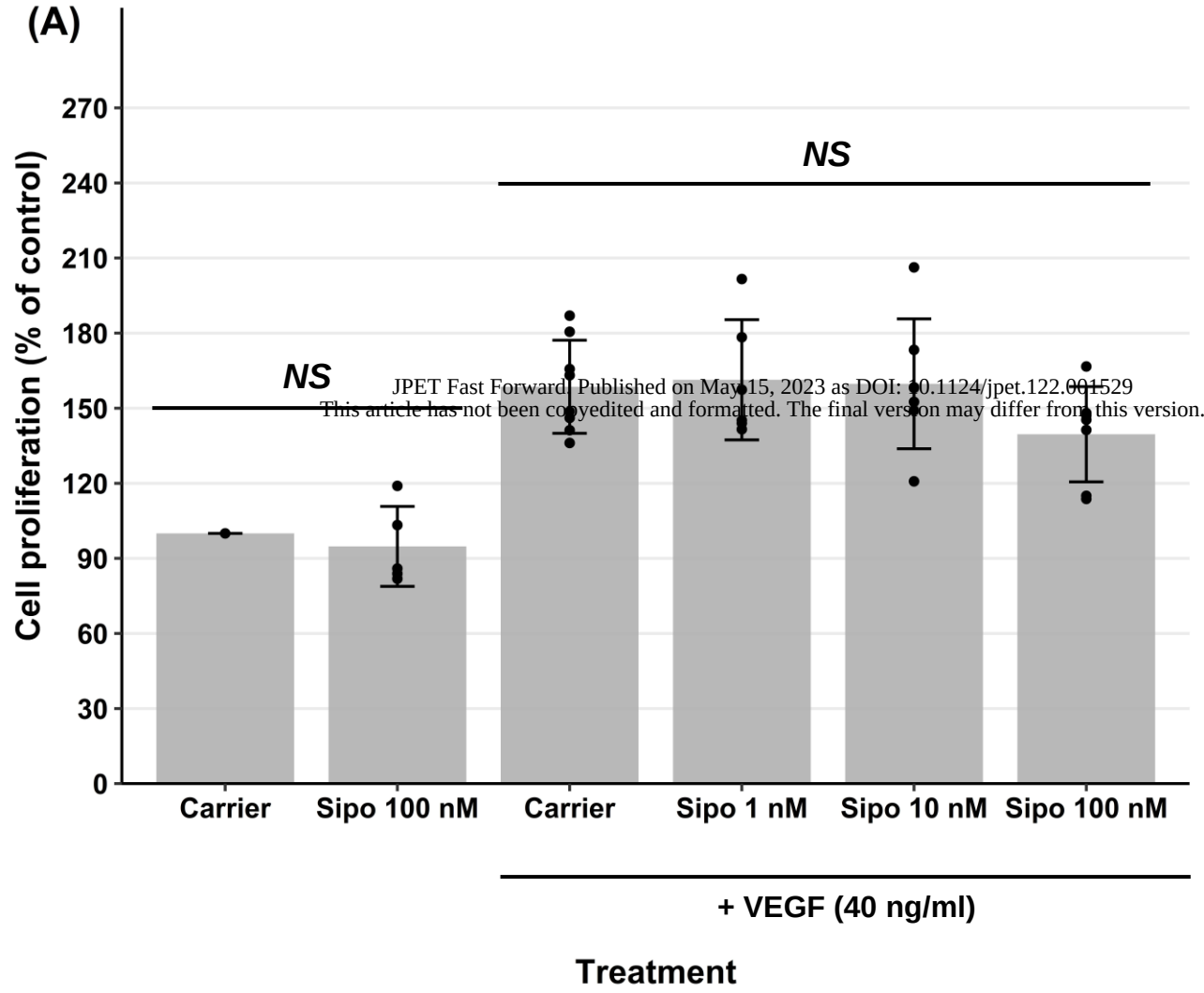


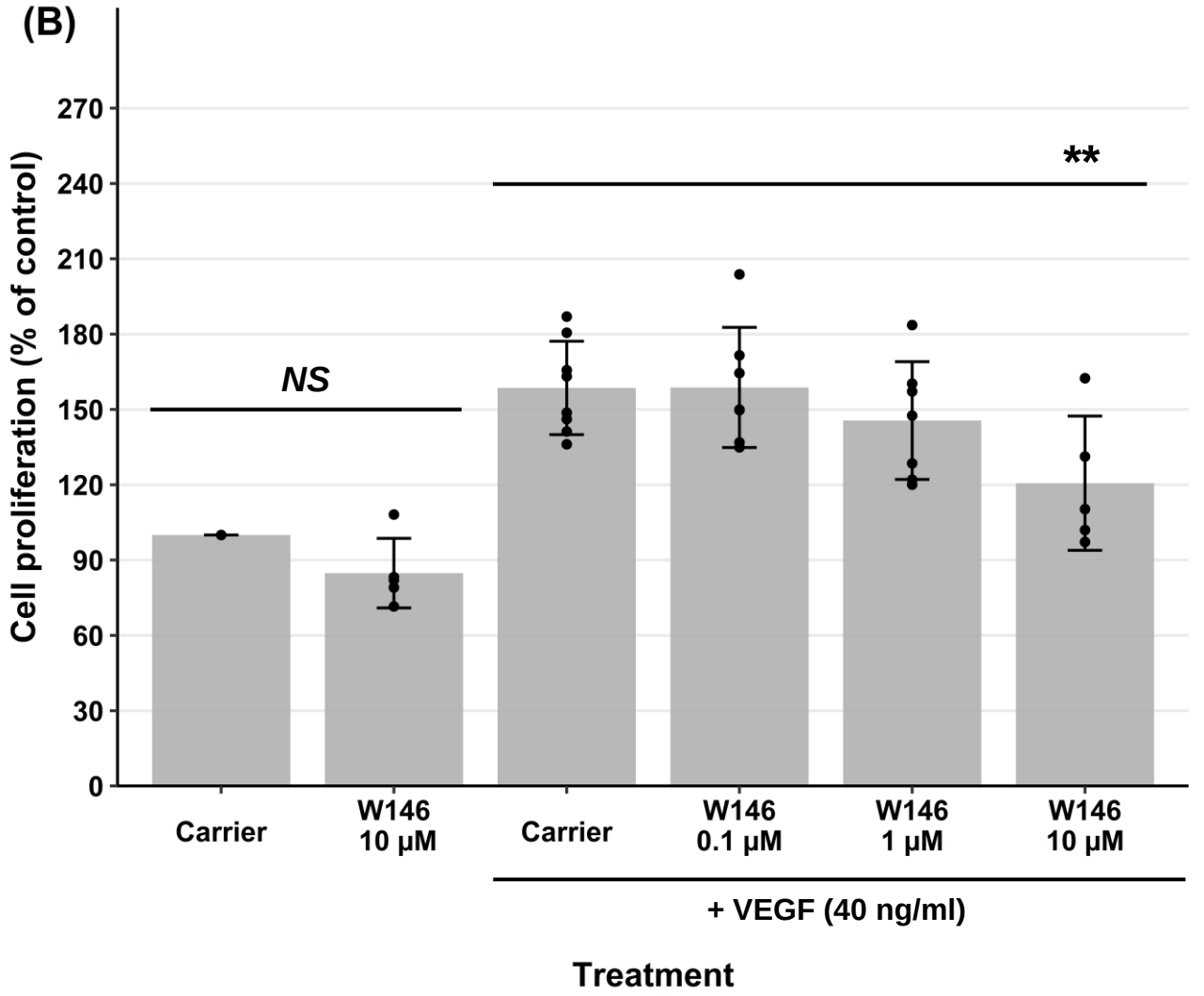
Fig. 4

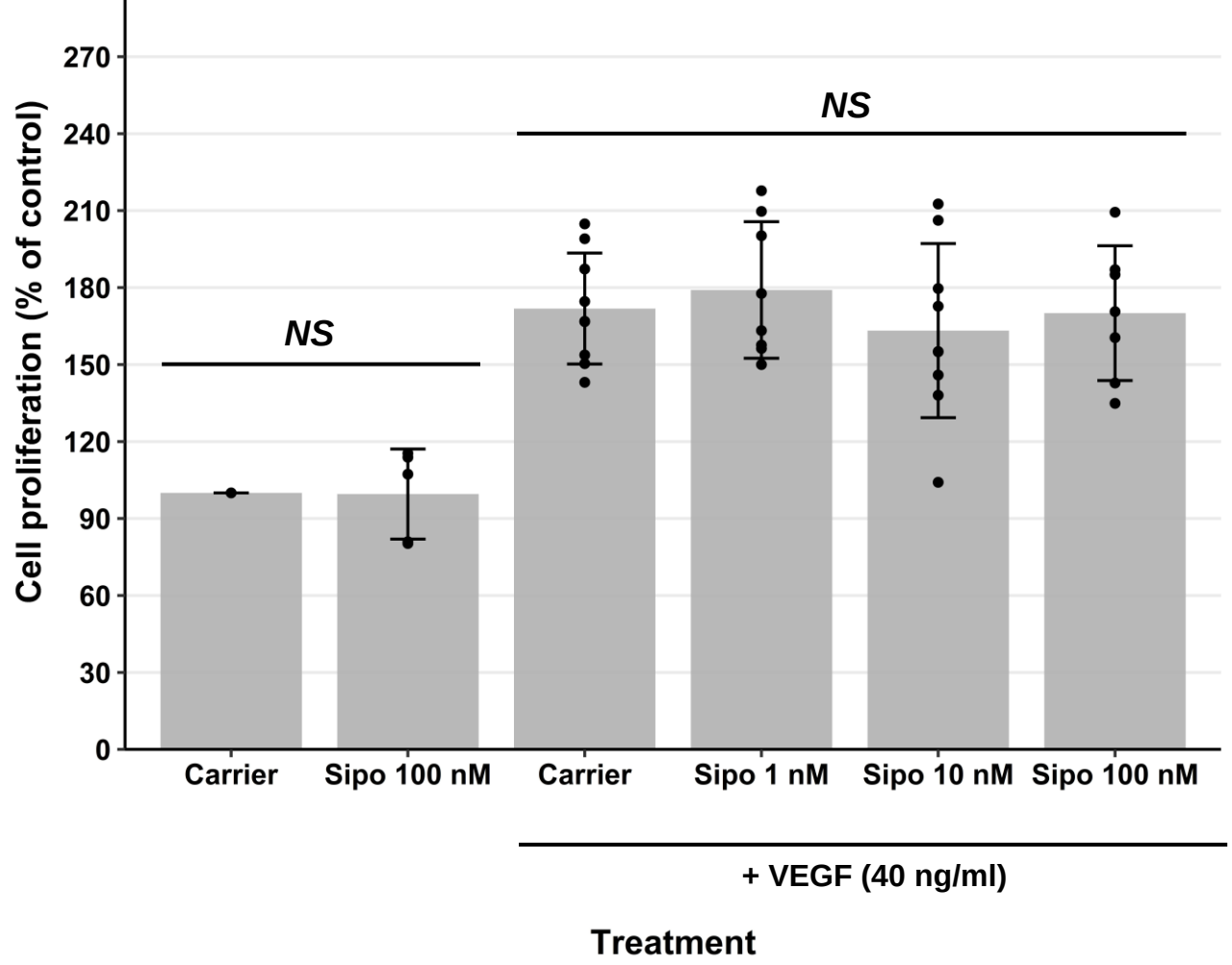
Downloaded from jpet.aspetjournals.org at ASPET Journals on June 6, 2023

JPET Fast Forward. Published on May 15, 2023 as DOI: 10.1124/jpet.122.001529
This article has not been copyedited and formatted. The final version may differ from this version.

Downloaded from jpet.aspetjournals.org at ASPET Journals on June 6, 2023







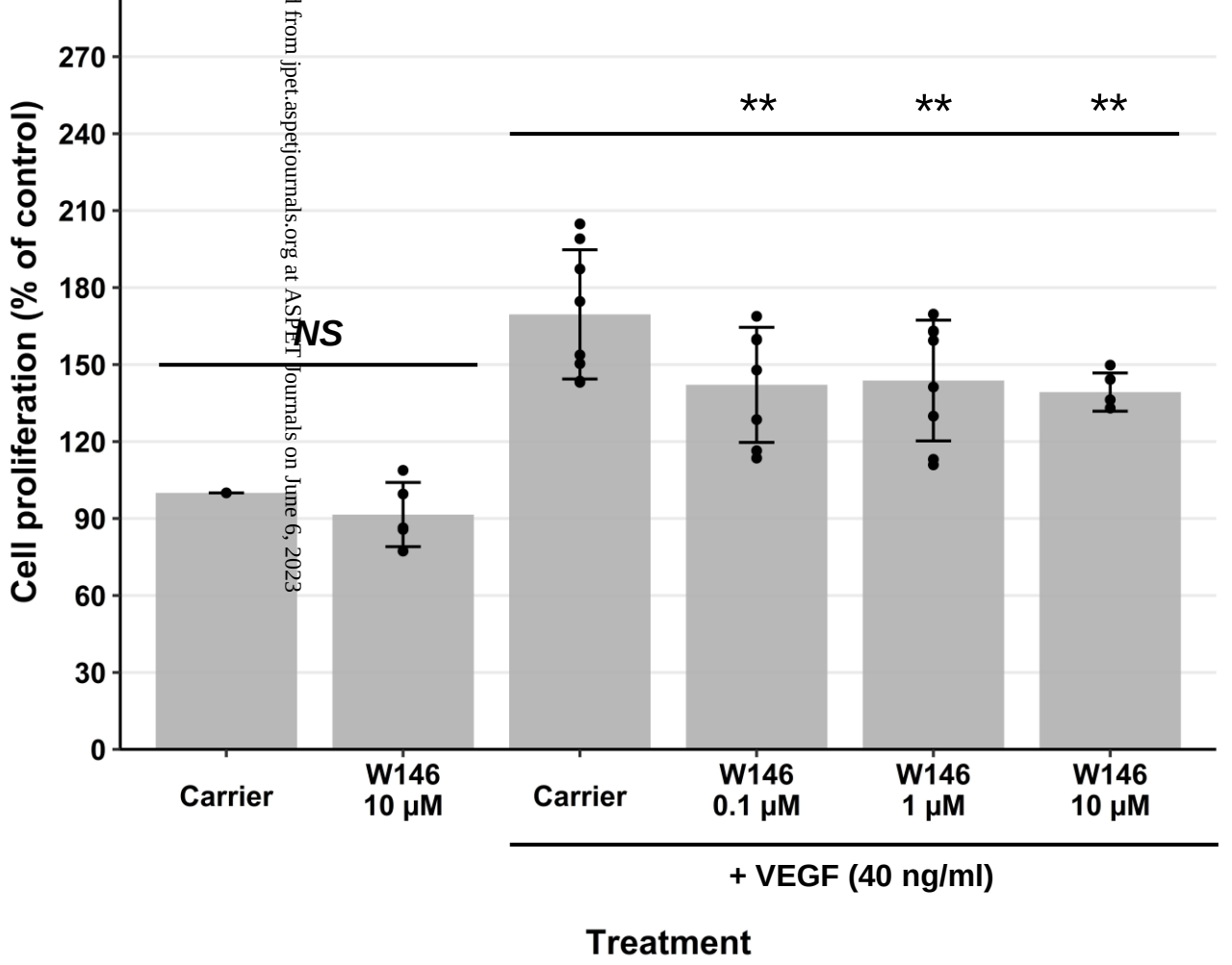
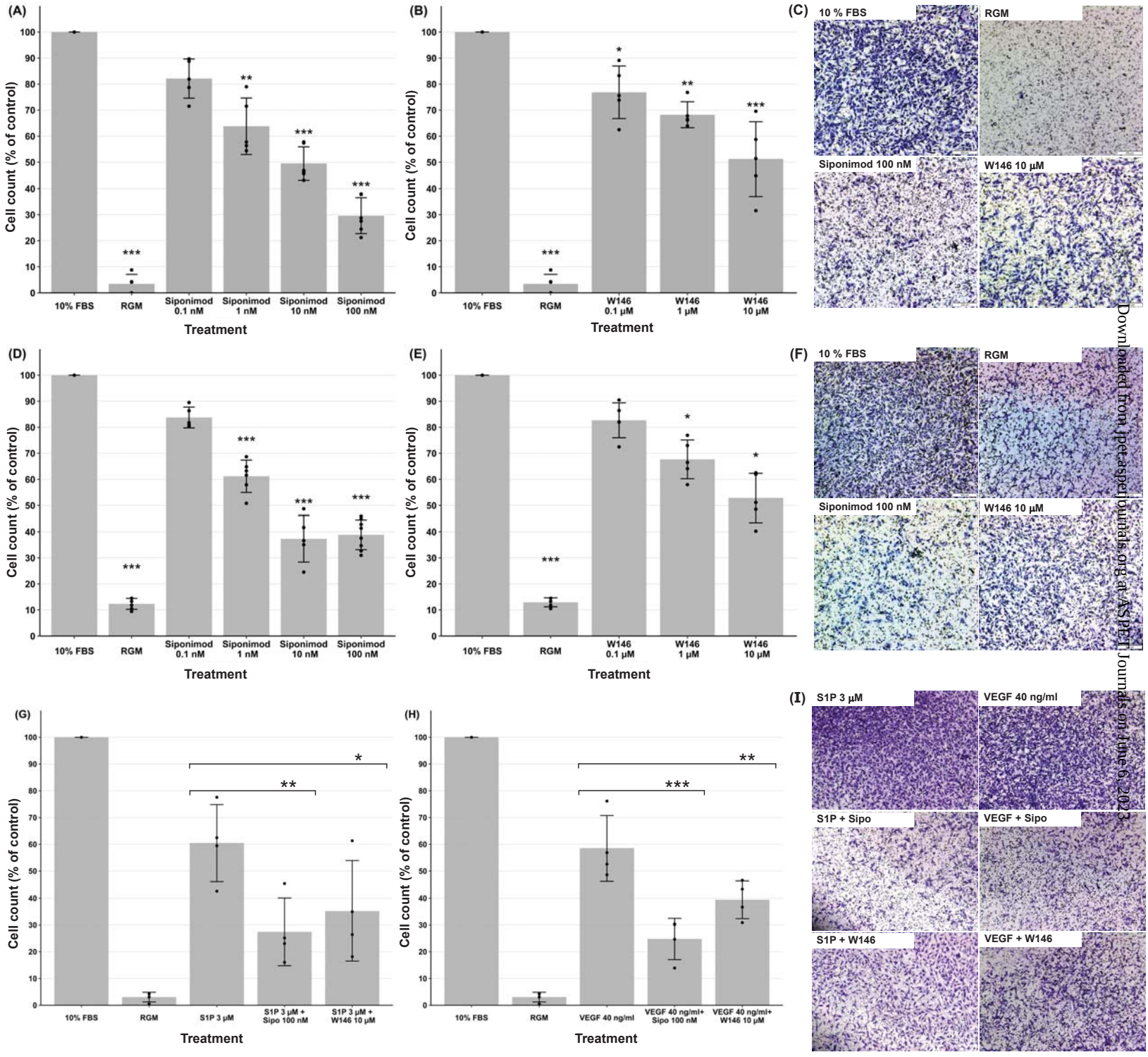


Fig. 5

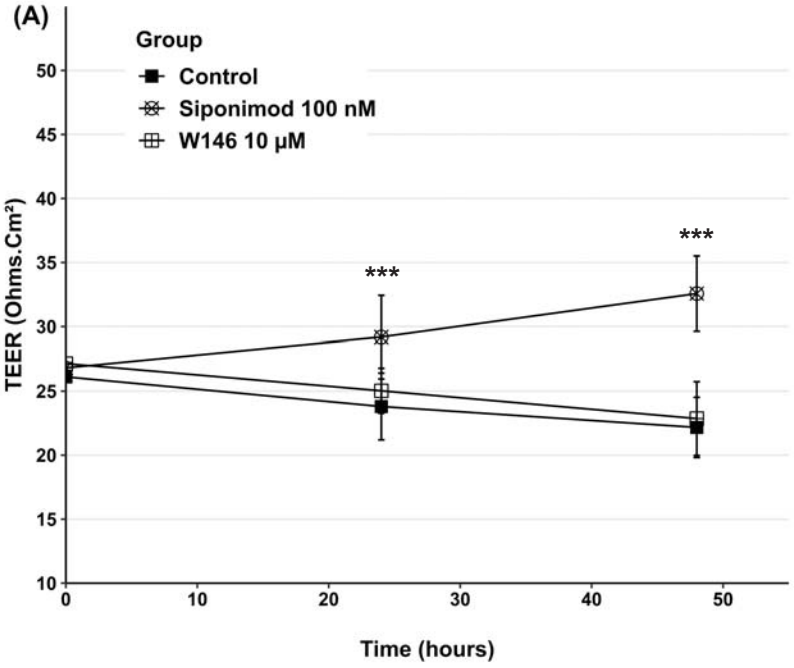
JPET Fast Forward. Published on May 15, 2023 as DOI: 10.1124/jpet.122.001529
This article has not been copyedited and formatted. The final version may differ from this version.

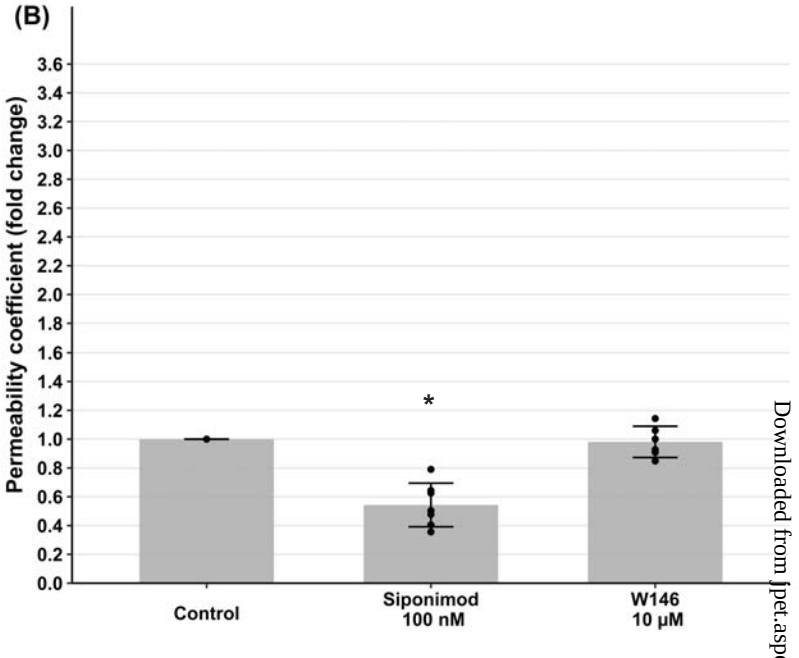


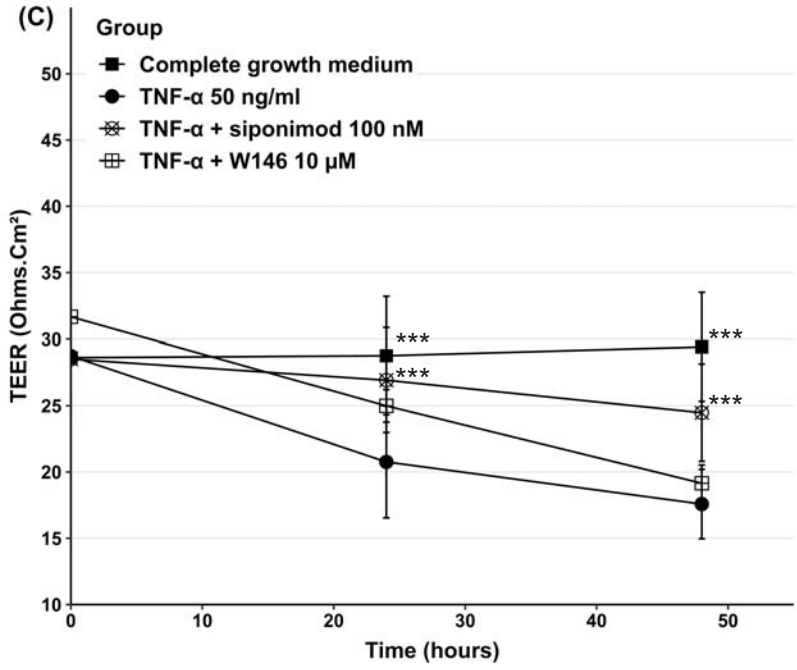
Downloaded from jpet.aspetjournals.org at ASPET Journals on June 6, 2023

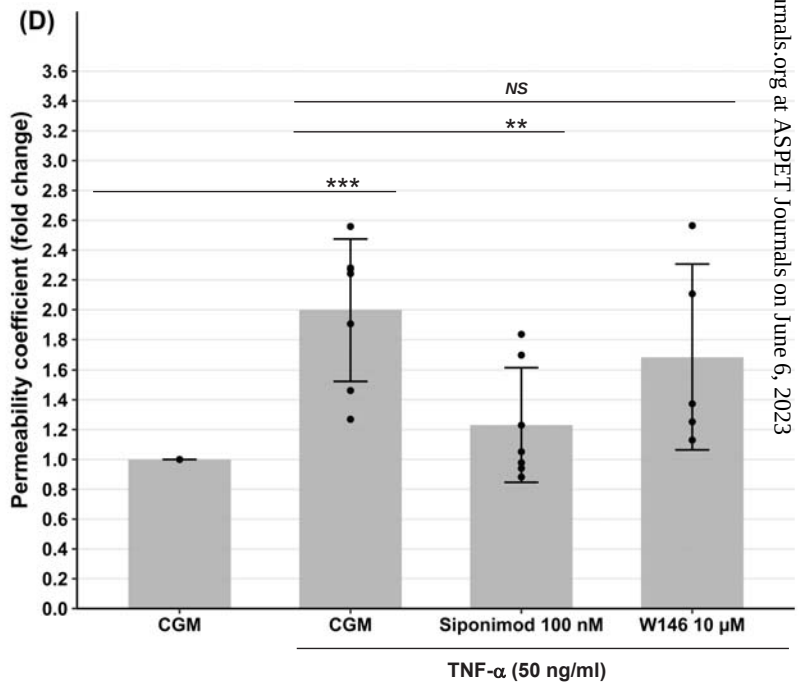
Fig. 6

JPET Fast Forward. Published on May 15, 2023 as DOI: 10.1124/jpet.122.001529
This article has not been copyedited and formatted. The final version may differ from this version.









Downloaded from jpet.aspetjournals.org at ASPET Journals on June 6, 2023

Fig. 7

JPET Fast Forward. Published on May 15, 2023 as DOI: 10.1124/jpet.122.001529
This article has not been copyedited and formatted. The final version may differ from this version.

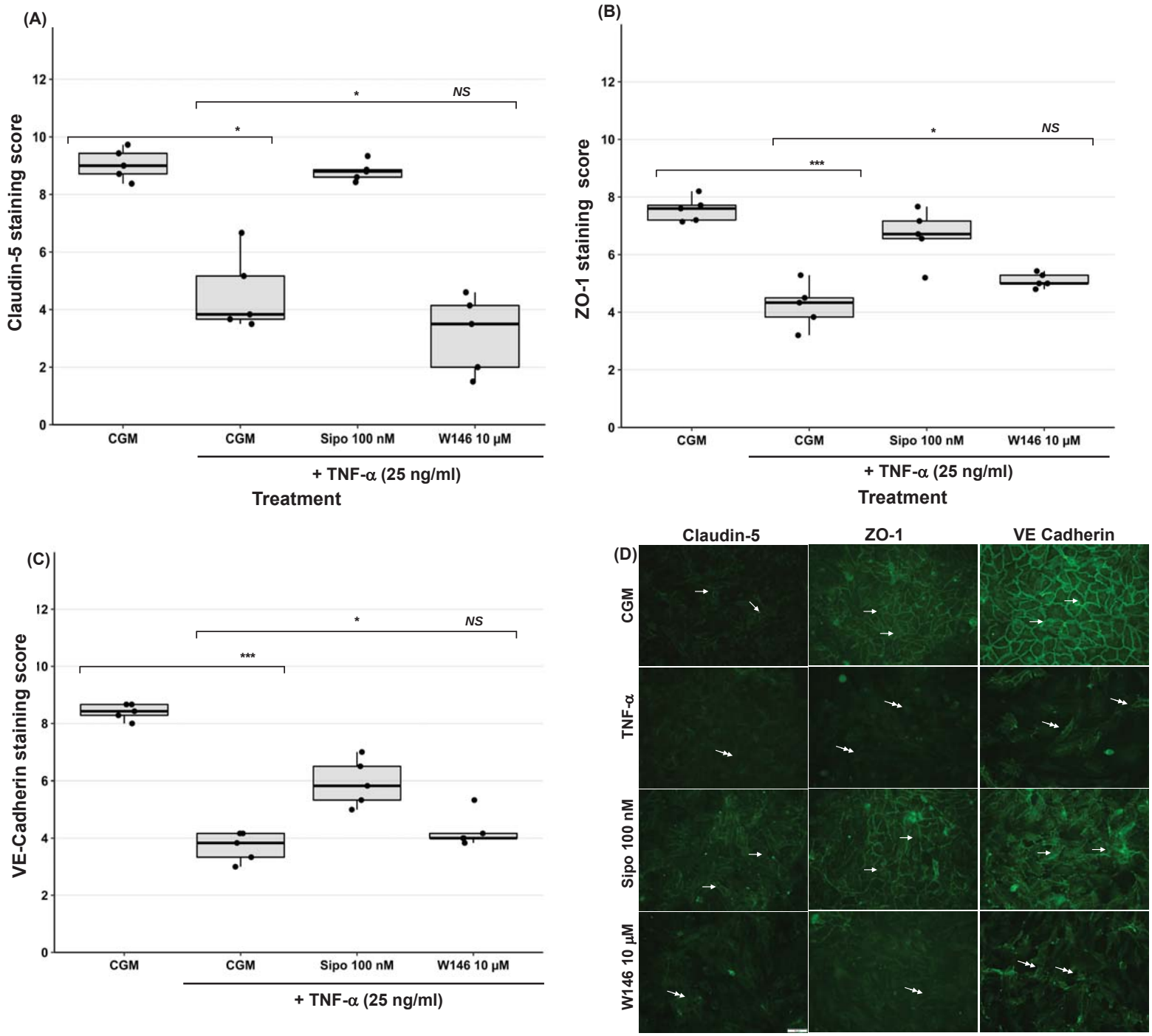
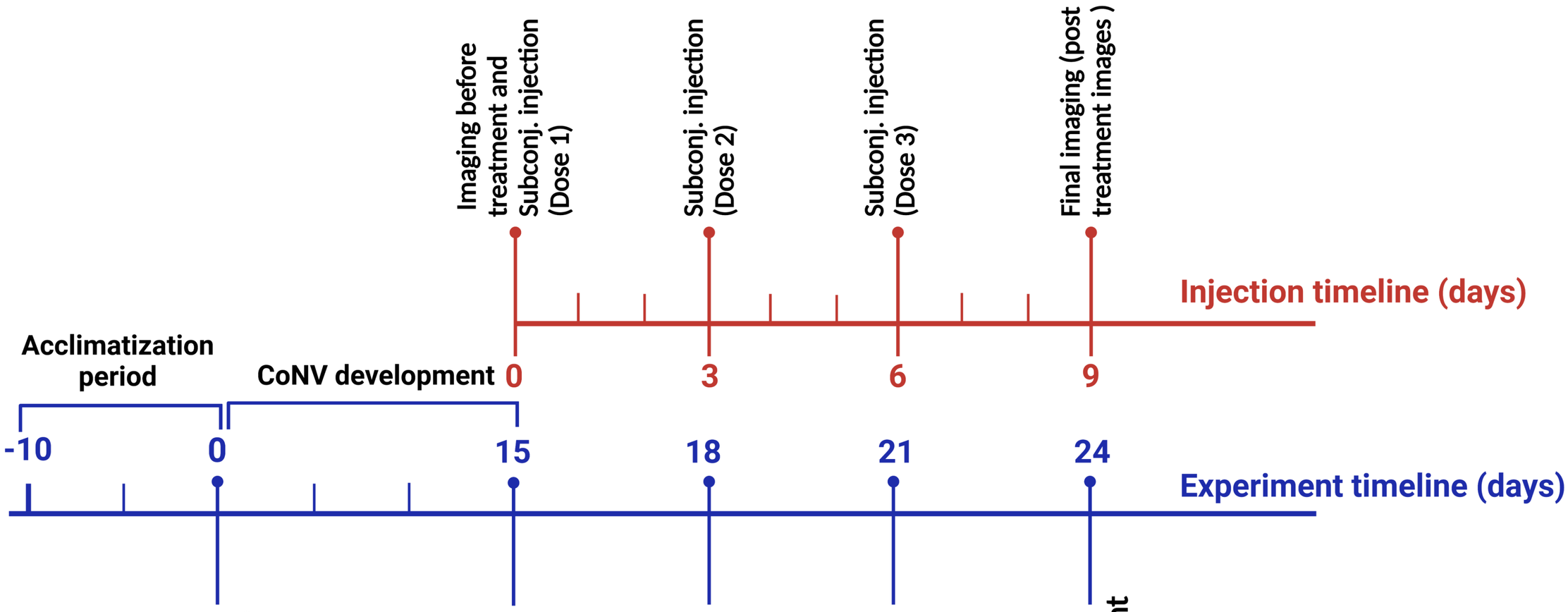


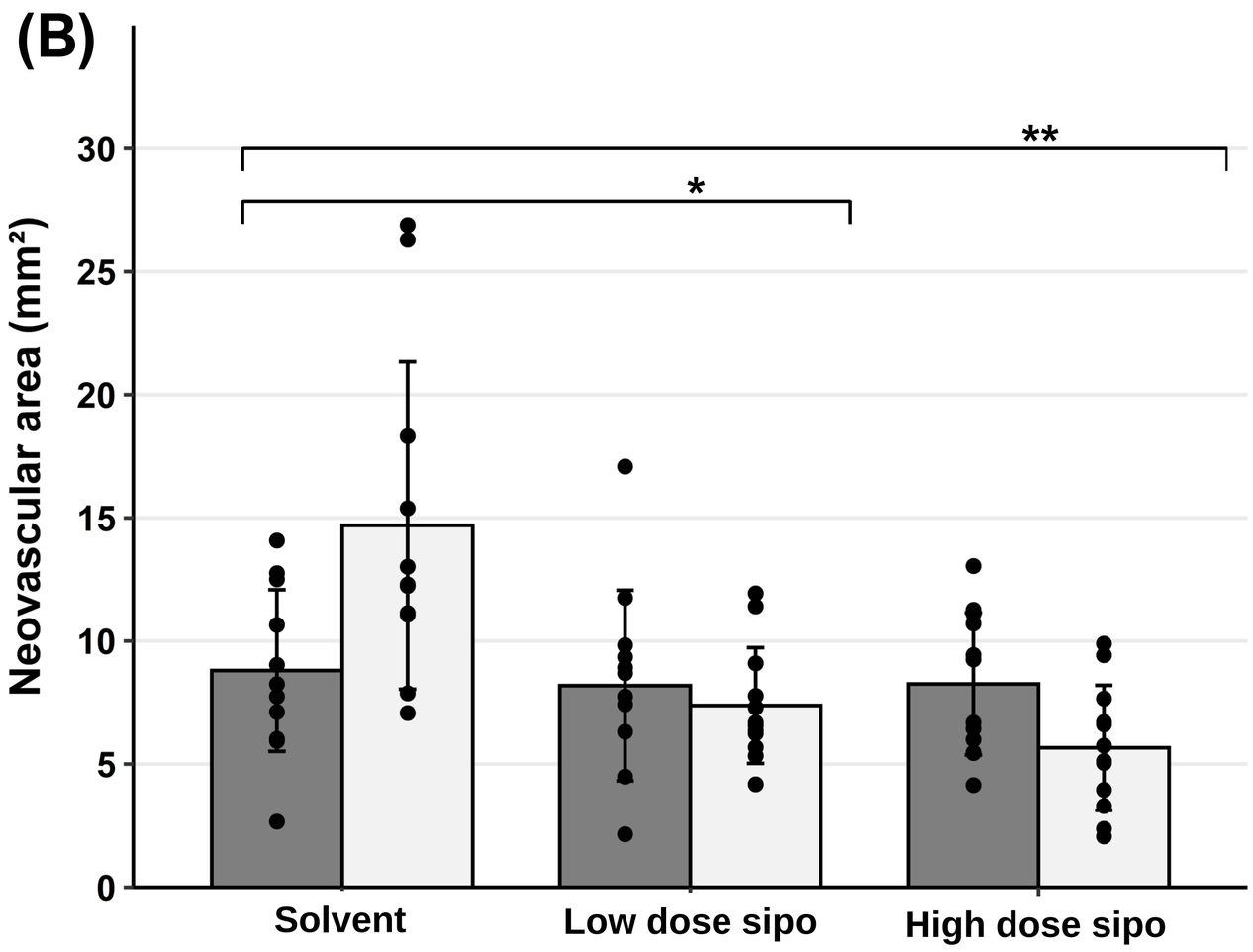
Fig. 8

Downloaded from jpet.aspetjournals.org at ASPET Journals on June 6, 2023

(A)

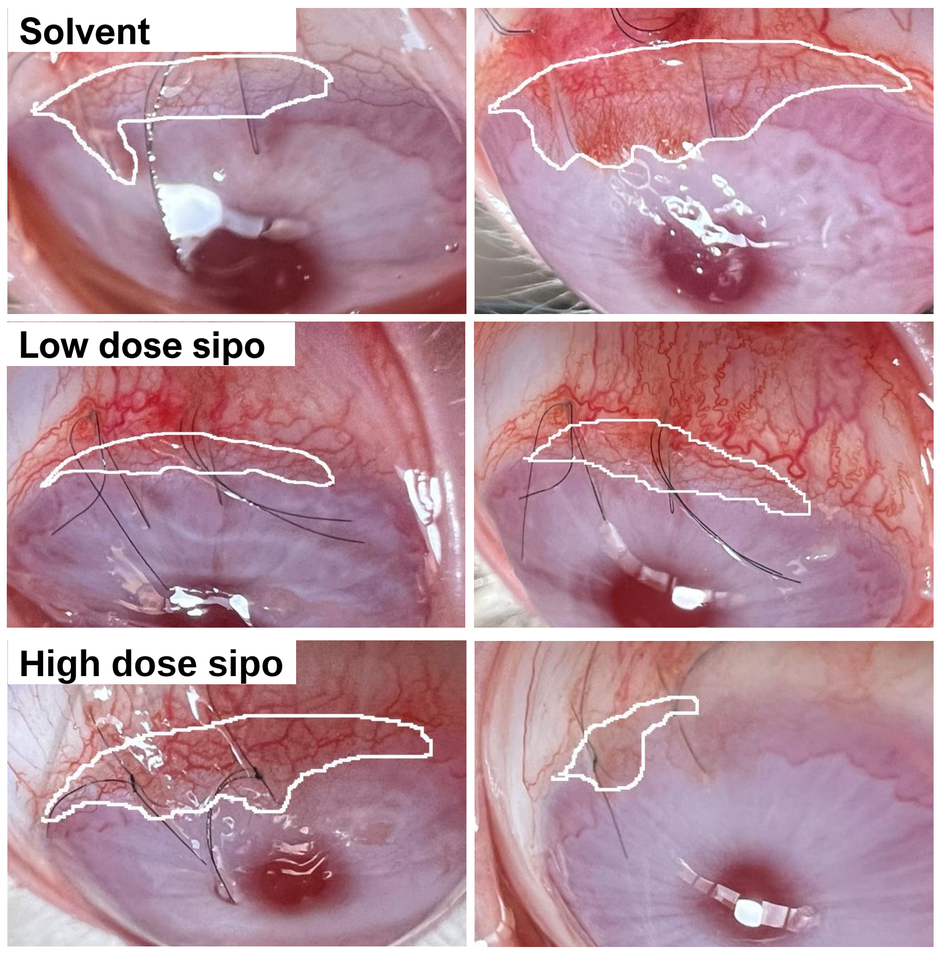


(B)



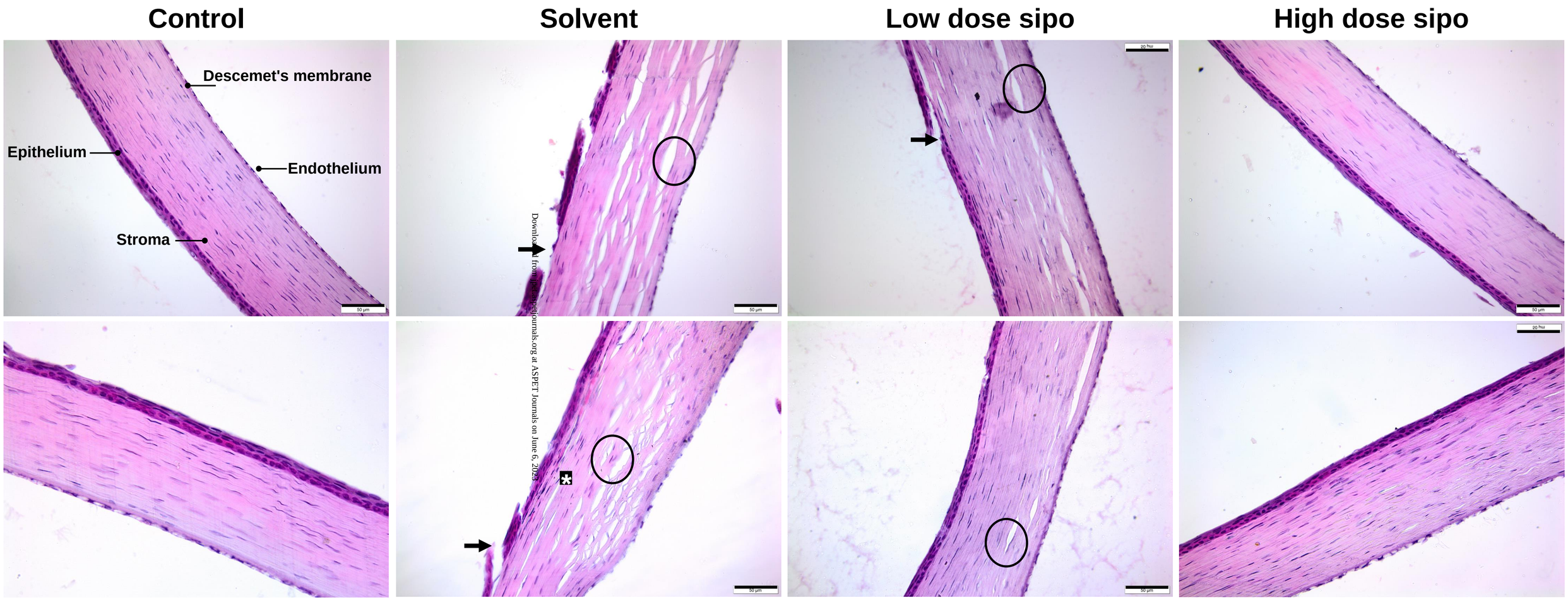


(C)



(D)

JPET Fast Forward. Published on May 15, 2023 as DOI: 10.1124/jpet.122.001529
This article has not been copyedited and formatted. The final version may differ from this version.



Downloaded from jpetjournals.org at ASPET Journals on June 6, 2023

Fig. 9

View publication stats